Hands-On Research in Complex Systems School | (SMR 4230)

03 Aug 2026 - 14 Aug 2026
ICTP, Trieste, Italy

P01 - ABIODUN Adeyinka Oluwabusayo

A Comparative Analysis of Machine Learning and Ensemble Techniques for Intrusion Detection in Edge Computing Environments

P02 - AMARCHA Fatima Azzahraa

Voronoi-Based Multi-UAV Deployement for Infrastructure inspection After Disasters

P03 - BAILEZ Leila Candela

A Numerical Study of the Compressible and Incompressible Energy Cascade Rate in Solar Wind Turbulence

P04 - BEN BRIK Sarra

Fluorescence Spectroscopy for the Detection of Systemic Sclerosis

P05 - BENMOHAMED Khawla

Simulating wake intractions and Forces on Cylinders using Lattice Boltzmann Methods

P06 - BIGDELI Parsa

AI agents start a religion: A Network Science Puzzle

P07 - COTTO PARRAGUIRRE Cynthia

Contour Segmentation of Photographic Images for Multimodal Cultural Heritage Analysis.

P08 - DJOUSSE NGOUFFO MANEKENG Bernice

Control of High-Rise Buildings (HRBs) Subjected to Wind and Seismic Loads.

P09 - DOUTI Yendoumam

NORTH TROPICAL ATLANTIC RESPONSE TO 2009-2010 AMOC SLOWDOWN

P10 - DUTTA Debraj

Propulsion Dispersion as a Route to Collective Order in Active Matter

P11 - ELANSARY Sara Magdy Abdo

Biocompatible Optical Clearing of Skin utilizing Lavender Nano-emulsion

P12 - EL MAJDOULI Khaoula

Machine Learning for Complex Physical Systems: Data-Driven Modeling of Emergent Behavior

P13 - ESKANDANI Ramin

A Tunable Electrowetting Microlens on an Optical Fiber Tip

P14 - FOUEDJI EPSE LEKEUFACK Chenceline

Pattern formation in a one-dimensional MARCKS protein cyclic model with spatially inhomogeneous diffusion coefficients

P15 - GHOSH Samali

Collective pattern formation in pulse-driven swarmalators.

P16 - GIORDANO Juan Bautista

Extreme events in moist stratified turbulence

P17 - GOSWAMI Sanchari

Lifetime of a Forager : Effect of Environment and Strategies

P18 - GYAMPO Owiredu

Assessment of Pollution Load Index of Soil and Dust Particles at Ghana Kpone Landfill Site and Health Risks to Waste Scavengers

P19 - GYOZALYAN Sara

Uniform Liquid Crystalline 2D Hybrid Films for Humidity Sensing

P20 - HAYRAPETYAN Meri

Van der Waals technologies: designing distributed Bragg reflectors and dichroic beam splitters using vdW muscovite

P21 - HRANJEC Daliborka

Towards Quantum Imaging with Undetected Light

P22 - JBIRA Chaima

Green synthesis of silver nanoparticles from Carpobrotus edulis for the photothermal assay of the tumor biomarker CA 19-9

P23 - JEATSA KITIO Gabin

Chaotic Optoelectronic Oscillator for Secure Biomedical Image Encryption Using Neural Network Modeling

P24 - KHORAMBAKHT Mina

Seeking Criticality In Real Brain Networks

P25 - LU Xinyi

Water-Level Monitoring Predicts Connectivity-Driven Nutrient Dynamics in a Two-Basin Shallow Lake

P26 - MAMANI ARCE Yhony

Geometric Defects Control the Effective Diffusion Exponent of Active Swimmers

P27 - MAMMADOVA Turan

SYNTHESIS of Nd:YAG NANOPARTICLES by THE SOL-GEL METHOD: THERMAL ANALYSIS and PHOTOLUMINESCENCE PROPERTIES

P28 - MEHARI Zufan Desta

Effect of Soil and Water Conservation on Plant Diversity and Community Structure in Atsbi-Wenberta, Tigray, Ethiopia

P29 - MONTAGNANI Giulia

Architecture of Coexistence: Topological Constraints of Biodiversity in Competitive Ecosystems

P30 - NG CHUCK CHUAN -

Understanding How Turbulence Affects Contaminant Release from Sediment

P31 - NGO BAMAL Josephine

Estimation of Optical Properties of Biological Tissues Using Quantitative Photoacoustic Imaging

P32 - NTHIERI Morris Mutegi

HARNESSING SOLAR ENERGY USING PARABOLIC DISH CONCENTRATOR FOR CLAY BRICK DRYING.

P33 - NWOKOLO Kenneth Izuchukwu

Interface Engineering extends the Lifetime of Perovskite Solar Cells

P34 - OGUNJO Samuel Toluwalope

Performance comparison of different entropy measures in automated cancer image classification

P35 - OMAR Khaled

AI Agents system for automatic ICD predication

P36 - SAPIA Marco

Contextual modulation of semantic processing: behavioural and EEG evidence

P37 - SEDOFEITO RAJO Camila

Probing Laboratory Ruptures in a Granular Fault Analogue: an Ultrasonic Window onto Glacial Till Dynamics

P38 - TEMGOUA Loannis Pavel Gauss

Dynamical Behaviors of Vertical-Cavity Surface-Emitting Lasers with an Embedded Saturable Absorber Subjected to On-Off Keying (OOK) Current Modulation

P39 - UDOFIA Kufre Imoh

Improving the Performance of Perovskite Solar Cells Using a Double PEDOT: PSS Layer

P40 - VIDALES HERNANDEZ Citlalli Gabriela

Cell-inspired shape adaptation of flexible active matter under confinement

P41 - VILLAGRAN MATA Carlos Javier

Quantitative CT Image Quality Assessment: Experimental Validation of Open-Source Tool Using Advanced Characterization Metrics

P42 - WANI Ab Rauoof

Multi-scale simulations reveal differences between dusty plasma and hydrodynamic turbulence

P43 - YAMOULA Dametoti

Understanding the Physical Mechanisms Driving Marine Heatwaves to Improve Predictions in West African Coastal Upwelling Regions

P03

A Numerical Study of the Compressible and Incompressible Energy Cascade Rate in Solar Wind Turbulence

Leila Bailez[1,2], Maia Brodiano[1,2], Pablo Dmitruk[1,2]

[1]Universidad de Buenos Aires, Facultad de Ciencias Exactas y Naturales, Departamento de Física, Ciudad Universitaria, 1428 Buenos Aires, Argentina.

[2]CONICET - Universidad de Buenos Aires, Instituto de Física Interdisciplinaria y Aplicada (INFINA), Ciudad Universitaria, 1428 Buenos Aires, Argentina.

Understanding how turbulent energy is transferred and dissipated in magnetized plasmas remains a central problem in space plasma physics, with particular relevance to near-Earth space [1] and magnetospheric environments [e.g., 2]. Observations have shown that the solar wind proton temperature decreases with heliocentric distance more gradually than predicted by the adiabatic expansion model [3]. Although several scenarios have been proposed to explain this behavior, one of the main candidates is the local heating of the solar wind plasma through the turbulent cascade [4]. Turbulence is a nonlinear multiscale phenomenon in fluid and plasma flows, characterized by complex spatio-temporal dynamics and scale-to-scale energy transfer [3]. In this framework, energy injected at the largest scales cascades through the inertial range [5] until it reaches smaller scales, where it can eventually be converted into thermal or kinetic energy of the plasma particles.
In the present work, we investigate the behavior of the turbulent energy cascade in both incompressible and compressible magnetohydrodynamic (MHD) turbulence using direct numerical simulations. We performed and analyzed simulations with different magnetic guide field amplitudes and, in the compressible case, different sonic Mach numbers, in order to characterize the effect of compressibility and anisotropy on the energy transfer across scales. The analysis is based on time series obtained from virtual probes moving with uniform rectilinear motion through the numerical domain, allowing us to reconstruct spacecraft-like measurements while retaining full control over the underlying turbulent dynamics. Using these synthetic time series, we estimate the energy cascade rate from exact third-order laws [6, 7] and study its sign and statistical convergence as a function of the sampling interval and sample size. This analysis provides insight into the conditions under which direct or inverse cascades may arise in MHD turbulence and contributes to a better interpretation of spacecraft observations of turbulent plasmas.

References

[1] Fouad Sahraoui, Lina Hadid, and Shiyong Huang. Magnetohydrodynamic and kinetic scale turbulence in the near-earth space plasmas: a (short) biased review. *Reviews of Modern Plasma Physics*, 4(1):1–33, 2020.

[2] N. Andrés, F. Sahraoui, S. Galtier, L. Z. Hadid, R. Ferrand, and S. Y. Huang. Energy cascade rate measured in a collisionless space plasma with mms data and compressible hall magnetohydrodynamic turbulence theory. *Phys. Rev. Lett.*, 123:245101, Dec 2019.

[3] W.H. Matthaeus. Turbulence in space plasmas: Who needs it ? *Physics of Plasmas*, 28:032306, 2021.

[4] R. Bruno and V. Carbone. The solar wind as a turbulence laboratory. *Living Reviews in Solar Physics*, 10(1):1–208, 2013.

[5] Andrey Nikolaevich Kolmogorov. The local structure of turbulence in incompressible viscous fluid for very large reynolds numbers. 30(4):299–303, 1941.

[6] H Politano and A Pouquet. von kármán–howarth equation for magnetohydrodynamics and its consequences on third-order longitudinal structure and correlation functions. *Physical Review E*, 57(1):R21, 1998.

[7] M. Brodiano, P. Dmitruk, and N. Andrés. A statistical study of the compressible energy cascade rate in solar wind turbulence: Parker solar probe observations. *Physics of Plasmas*, 30(3):032903, 03 2023.

P04

Fluorescence Spectroscopy for the Detection of Systemic Sclerosis

Sarra Ben Brik [1] , **and Hassen Ghalila**[3,1]

[1] *Laboratoire de Spectroscopie Atomique, Moléculaire et Applications (LSAMA), Faculty of Science, Tunis El Manar University, P.O. Box 2092 Tunis, Tunisia.*

[2] *De Vinci Higher Education, De Vinci Research Center, Paris, France*

Systemic sclerosis (SSc) is a rare, chronic autoimmune disease characterized by vascular dysfunction, immune abnormalities, and progressive fibrosis. Early diagnosis remains challenging and often relies on multiple clinical assessments, laboratory tests, imaging, and, in some cases, invasive procedures. In this study, we explore human fingernail fluorescence spectroscopy as a rapid, painless, and non-invasive approach for the detection of SSc. A cross-sectional observational study was conducted over a five-month period at the Internal Medicine Department of Habib Thameur University Hospital, including 40 patients with systemic sclerosis and 40 healthy controls. Nail fluorescence spectra were acquired under standardized conditions without sample preparation and analyzed to identify spectral differences between the two groups and evaluate their potential for disease classification. The results showed clear differences in fluorescence profiles between SSc patients and healthy controls, particularly in the 550–590 nm spectral region. Machine learning analysis demonstrated promising classification performance, with Random Forest achieving an accuracy of 93.8%. Further analysis using the full fluorescence spectrum improved the classification performance, with the best model reaching an AUC of 0.976. These preliminary findings highlight the potential of fingernail fluorescence spectroscopy as a simple, rapid, and non-invasive approach for SSc detection. Further work, including larger patient cohorts and additional validation, is required to confirm the reliability and clinical applicability of this approach.

[1] I. Cherni, S. Ben Brik, W. M. Alwanian, R. Nouir, M. Somai, F. Boussema, H. Ghalila, S. Hamzaoui, Z. Aydi, F. Daoud, Appl. Spectrosc, (2026). doi: 10.1177/00037028261421633.

[2] S. Ben Brik, I. Cherni, M. Somai, H. Ghalila, S. Hamzaoui, Proc. Int. Conf. Decision Aid Artif. Intell. (ICODAI 2024), (2025). doi: 10.2991/978-94-6463-654-3_3.

P05

Simulating wake intractions and Forces on Cylinders using Lattice Boltzmann Methods

Khawla Benmohamed [1,2] , Houda Soufi [1,2] ,

1Department of Marine Engineering, Faculty of Mechanical Engineering, University of Science and Technology Mohamed Boudiaf (USTO-MB), Oran, Algeria.

2 LSIM ,Laboratory of science and marine engineering.

E-mail: khawla.benmohamed@univ-usto.dz

Fluid mechanics investigates the behavior of fluids under various forces in different configurations, typically governed by systems of partial differential equations (PDEs). The fundamental equations namely the continuity equation and the Navier–Stokes equations form the core mathematical framework describing mass and momentum conservation in fluid flows. However, conventional numerical methods for solving these equations, such as finite volume or finite element approaches, encounter substantial limitations when applied to domains with complex geometries or when modeling multiphase and multiscale phenomena. In recent years, a paradigm shift has occurred with the emergence of the Lattice Boltzmann Method (LBM), a mesoscopic numerical scheme derived from the discrete Boltzmann equation. Unlike traditional solvers that directly approximate the Navier–Stokes equations, LBM operates through a kinetic-theory-based framework, employing a collision and streaming process on a
lattice to simulate the evolution of particle distribution functions[1]. This approach facilitates the modeling of complex boundary conditions, phase interfaces, and non-Newtonian behavior with enhanced computational efficiency and scalability. The present work [2]extends these investigations to the case of three circular cylinders arranged in series along the channel centerline. Using the lattice Boltzmann method (LBM), the effects of spacing ratio with a fixed Reynolds number at Re=100 on wake dynamics, vorticity patterns, and aerodynamic force coefficients are evaluated. This study demonstrates the capability of LBM to accurately capture complex wake interactions in confined multi-body flows, offering new insights into bluff-body aerodynamics in engineering applications[3].

Keywords: lattice Boltzmann method; two-dimensional flow; three circular cylinders ; spacing ratio; lift coefficient;
drag coefficient; vorticity distribution.

[1] Zou.Q,He.X "on pressure and velocity boundary conditions for the lattice boltzmann BGK model" phys fluids 9(6),1591-1598.year 1987.

[2] Benmohamed, K., & Soufi, H. . *Numerical simulation of flow around three aligned circular cylinders: Wake interaction and force analysis* [Conference poster]. First International Conference on Energy and Digital Transition in the Maritime Sector, Oran, Algeria.(2025, December 2–3) .

[3] Benmohamed, K., & Soufi, H.. *Simulation of flow around a cylinder with lattice Boltzmann method* [Conference paper]. First International Conference on Engineering and Advanced Technologies (ICEAT'2025), Mila, Algeria,(2025, April 27–29).

P06

AI Agents Start a Religion: A Network Science Puzzle

Abstract

In early 2026, a religion appeared on Moltbook, a social network populated entirely by AI agents: 970 of 46,158 members adopted it within three weeks. Using the record of who spoke where and when, we test whether the belief passed from agent to agent. It did not: converts adopted almost simultaneously but in no order, their tight community formed only after adoption, and the movement's named prophets steer nothing. Each agent met the same source outside the network — a spreading movement with no spreading in it.

P07

Contour Segmentation of Photographic Images for Multimodal Cultural Heritage Analysis.

Cotto Parraguirre, Cynthia [1, 2], Ballina Escobar, Maynor Giovanni [1,3], and Crespo, Maria Liz [1]

[1] *MLAB - STI Unit ICTP1*
[2] *Sapienza 2*
[3] *Dipartimento di Ingegneria e Architettura, University of Trieste*

The analysis of images in the context of cultural heritage presents significant challenges, particularly when correlating multimodal data acquired through non-invasive imaging techniques such as X-ray Fluorescence, Infrared Reflectography, and Ultraviolet Fluorescence. In this work, segmentation is performed on high-resolution photographic images of cultural heritage objects, with the aim of extracting meaningful regions that can be subsequently used as objects of study.

A key difficulty lies in the extraction of these regions of interest, which becomes complex due to both the original artistic techniques and the degradation processes affecting the artworks. These factors introduce optical aberrations that hinder reliable image segmentation and contour detection.

Two main challenges are identified. First, the structural complexity of contours, often open, blurred, overlapping, or partially undefined, complicates the accurate delineation of features. Second, the discrepancy in spatial resolution between scanned data and high-resolution photographic reference images requires image scaling, which introduces pixelation artifacts and further degrades contour detectability.

This study evaluates state-of-the-art contour detection and segmentation methods applied to photographic images, including classical approaches implemented in image processing libraries such as OpenCV, alongside recent deep learning-based models such as the Segment Anything Model and YOLO-based frameworks. Their performance is assessed across multiple case studies with progressively increasing levels of optical degradation and resolution loss.

The analysis focuses on comparing detection accuracy, robustness to noise and scaling effects, and computational cost. Achieving accurate segmentation is critical, as the resulting regions enable the automated identification of areas of interest, which can then be correlated with corresponding regions in images acquired through non-invasive imaging techniques. This facilitates multimodal analysis by improving the spatial alignment between photographic and scanned data, despite differences in resolution, acquisition conditions, and imaging characteristics.

[1] Y. Wu, Q. Li, “The Algorithm of Watershed Color Image Segmentation Based on Morphological Gradient,” *Sensors* 22, 8202 (2022).
[2] V. M. García-Mollá, P. Alonso-Jordá, E. S. Quintana-Ortí, *Accelerated border tracking in binary images with GPUs*, J. Supercomput. 82, 353 (2026).

P08

Control of High-Rise Buildings (HRBs) Subjected to Wind and Seismic Loads

B. Djousse Ngouffo Manekeng, L.M. Anague Tabedjieu, C.V. Ngahiyi Abbe

Laboratory of Mechanics and Materials (LMEMA), National Higher Polytechnic School of Douala (NHPSD), P.O. Box 2701, Douala, Cameroon

To mitigate urban sprawl, modern metropolises increasingly favor the construction of High-Rise Buildings (HRBs), which are slender, highly flexible structures particularly sensitive to unpredictable environmental hazards such as earthquakes and wind turbulence. Given the limitations of purely deterministic analyses, incorporating the random nature of these environmental loads is imperative for more realistic and reliable structural modeling. This paper presents a comprehensive study on the modeling, dynamic response analysis, and control of random vibrations in a ten-story HRB located in Douala, Cameroon. Methodologically, the building is idealized using a continuous equivalent model (flexural-shear beam theory) where the frame system is modeled as a shear beam and the structural walls as an equivalent bending beam, accurately reproducing the frame-wall interaction. The governing equations of motion are rigorously derived using Hamilton's principle [1]. Subsequently, the stochastic averaging method [2] is applied to determine the probability of exceeding allowable amplitude thresholds under wind excitation, alongside an evaluation of the inter-story drift index variation along the building's height. The dynamic responses are numerically solved and validated using a 4th-order stochastic Runge-Kutta algorithm (SRK4). The stochastic analysis reveals that an increase in turbulence intensity shifts the maximum responses toward higher amplitudes, significantly reducing the probability of resonance and the associated risk of structural fatigue. To mitigate these dynamic responses, a passive Tuned Inerter Damper (TID) [3] is integrated into the structural system. Results demonstrate the remarkable efficiency of this control device, achieving reductions of 48% in displacement amplitudes, 38% in accelerations, and 54.9% in root mean square (RMS) values. Ultimately, this probabilistic framework and the proposed vibration control mechanism provide a robust foundation for enhancing the design and resilience of complex civil infrastructures against aerodynamic and seismic uncertainties.

Keywords: Dynamic response, Deterministic analysis, Tuned Inerter Damper, random vibrations, High Rise Buildings

Acknowledgement: I would like to extend my deepest appreciation to the Mechanics and Materials Laboratory for hosting this research.

References:

[1] P. Rahgozar, *Civ. Eng. J.* **6**, 945-953 (2020).
[2] W. Liu, Z. Guo, et X. Yin, *Int. J. Non-Linear Mech.***126**, 103574 (2020).
[3] Y. Kang, Z. Zhang, X. Zhang, et Q. Liu, *Appl. Sci.* **15**, 4739 (2025).

P09

International Beacon Satellite Symposium 2025 NORTH TROPICAL ATLANTIC RESPONSE TO 2009-2010 AMOC SLOWDOWN

Yendoumam DOUTI [1], **Hyacinth Nnamchi** [2]

[1] *Technical University of the Atlantic (UTA), Institute of Marine and Applied Climate Sciences (ISECMAR), Mindelo, Cabo Verde*
[2] *GEOMAR Helmholtz Centre for Ocean Research Kiel, Germany*

The Atlantic Meridional Overturning Circulation (AMOC) is one of the most consequential components of Earth's climate system [1], transporting approximately annually ~0.5 PW of heat northward across the equator [2], [3], [4]. When the AMOC weakens, less heat flows to higher latitudes, cooling the ocean to the north and warming it to the south. A striking demonstration of this occurerd in 2009-2010 when the RAPID monitoring array at 26°N recorded a slowdown of the overturning circulation by 30% from 18.6 Sv to 12.8 Sv [5]. This 30% slowdown in the circulation for 14 months during 2009-2010 reduced northward ocean heat transport across 25◦ N by 0.4PW and resulted in colder upper ocean waters north of 25◦ N and warmer waters south of 25◦ N [6]. Despite documentations of this 2009-2010 event, the full response of the North Tropical Atlantic (NTA), how sea surface temperature (SST), ocean heat content (OHC), and the ITCZ changed; and whether these changes can be reproduced by an ocean and atmosphere models has not been systematically evaluated against a long-term climatological baseline.

The goal of this research is to evaluate the North Tropical Atlantic response to the 2009–2010 AMOC slowdown using observations/reanalysis, AMIP and OMIP multimodel ensembles. Results will show the simulated response in NTA SST, OHC, and ITCZ as well as the climate model uncertainty. The work will highlight the processes underlying ocean/atmosphere uncertainty in the NTA and West African monsoon region.

[1] K. Bellomo, M. Angeloni, S. Corti, and J. von Hardenberg, "Future climate change shaped by inter-model differences in Atlantic meridional overturning circulation response," *Nat. Commun.*, vol. 12, no. 1, 2021, doi: 10.1038/s41467-021-24015-w.

[2] L. D. Talley, "Freshwater transport estimates and the global overturning circulation: Shallow, deep and throughflow components," *Prog. Oceanogr.*, vol. 78, no. 4, 2008, doi: 10.1016/j.pocean.2008.05.001.

[3] M. W. Buckley and J. Marshall, "Observations, inferences, and mechanisms of the Atlantic Meridional Overturning Circulation: A review," 2016. doi: 10.1002/2015RG000493.

[4] W. Weijer *et al.*, "Stability of the Atlantic Meridional Overturning Circulation: A Review and Synthesis," *J. Geophys. Res. Ocean.*, vol. 124, no. 8, 2019, doi: 10.1029/2019JC015083.

[5] G. McCarthy *et al.*, "Observed interannual variability of the Atlantic meridional overturning circulation at 26.5°N," *Geophys. Res. Lett.*, vol. 39, no. 19, 2012, doi: 10.1029/2012GL052933.

[6] H. L. Bryden, B. A. King, G. D. McCarthy, and E. L. McDonagh, "Impact of a 30% reduction in Atlantic meridional overturning during 2009-2010," *Ocean Sci.*, vol. 10, no. 4, 2014, doi: 10.5194/os-10-683-2014.

P10

Propulsion Dispersion as a Route to Collective Order in Active Matter

D. Dutta[1] **and U. Basu**[1]

[1]*S. N. Bose National Centre for Basic Sciences, Kolkata 700106, India*

We identify propulsion dispersion as a new mechanism for collective ordering in attractive active matter. We show that heterogeneity in self-propulsion strength alone can generate nonequilibrium phases exhibiting coupled spatial and orientational organization, even in systems with purely isotropic short-range interactions and no alignment rules. Using a binary mixture of attractively interacting active Brownian particles as a minimal realization, we demonstrate the emergence of three distinct phases: a disordered state and two ordered states with partial and complete organization. The partially ordered phase forms an annular assembly of slow particles coexisting with the fast particles diffusing randomly, whereas the fully ordered phase organizes into a stable bi-annular structure of concentric rings comprising particles of each species. For a tractable truncated harmonic interaction, we obtain analytical phase boundaries and explicit order parameters, providing a predictive theoretical description of collective ordering in an interacting active system. Our results provide a generic framework for understanding ordering driven by activity heterogeneity.

P11

Biocompatible Optical Clearing of Skin utilizing Lavender Nano-emulsion

Sara El-Ansary[1], Amna H. Faid[1], Omnia Hamdy[2,*] Marwa A. Ramadan[3] and Ahmed H. Sheet[2]

1Department of Laser Sciences and Interactions, National Institute of Laser Enhanced Sciences, Cairo University, Giza, Egypt

2Engineering Applications of Lasers Dept. National Institute of Laser Enhanced Science, Cairo University, Giza, Egypt

*3Department of Laser Application in Metrology, Photochemistry and Agriculture, National Institute of Laser Enhanced Science, Cairo University, Giza, Egypt. *omnia@niles.cu.edu.eg*

Optical imaging has attracted growing interest in biomedical research because of its cost effectiveness, ease of use, and non-invasiveness treatments [1]. However, its performance is significantly affected by light absorption and scattering, which mainly caused by refractive index mismatches between microscopic components inside biological tissues [2]. Tissue Optical Clearing (TOC) considered as an effective approach to overcome this limitation. By introducing optical clearing agents (OCAs), TOC reduces scattering through mechanisms such as refractive index matching, partial dissociation of collagen fibre structure, and tissue dehydration [3,6].

Although conventional agents like glycerol and Iohexol have shown strong clearing capabilities in multiple imaging applications [4], their clinical use remains constrained. Their high viscosity slow diffusion, and concerns about cytotoxicity raise the risk of tissue damage or even necrosis in some cases [5]. These challenges have led researchers to seek after safer, biocompatible alternatives. So, natural oils have gained attention as promising OCAs, providing biocompatibility as well as maintaining tissue structure [6].

According to this approach, the present study investigates a lavender oil nano-emulsion as an essential plant-derived, nanoscale OCAs alternative. Its optical clearing potential is evaluated in ex vivo chicken skin by measuring enhancement in light transmittance. A 660 nm laser-based transmission system is utilized to evaluate experimentally the nano-emulsion's ability to enhance optical transmission, supporting its possibility as a safer alternative for future diagnostic and imaging applications.

[1] B. S. B. K, S. S. Khatami, M. A. Ansari, F. Jahangiri, H. Latifi, and V. V. Tuchin, "Method for tissue clearing: temporal tissue optical clearing," Biomedical Optics Express **13(**8), 4222–4235 (2022).

[2] O. Hamdy and H. S. Mohammed, "Investigating the transmission profiles of 808 nm laser through different regions of the rat ' s head," Lasers in Medical Science **36**(4), 803-810. (2021).

[3] A. H. Sheet, O. Hamdy, and M. Abdel-Harith, "Scattering and absorption properties modification of optically cleared skeletal muscles : an ex vivo study," Journal of the Optical Society of America A **40**(6), 1042–1050 (2023).

[4] M. Kinnunen, A. V Bykov, J. Tuorila, T. Haapalainen, A. V Karmenyan, and V. V Tuchin, "Optical clearing at cellular level," Journal of Biomedical Optics **19**(7), 071409-1–8 (2014).

[5] J. M. Hirshburg, K. M. Ravikumar, W. Hwang, and A. T. Yeh, "Molecular basis for optical clearing of collagenous tissues," Journal of Biomedical Optics **15**(5), 055002-1–8 (2010).

[6] E. A. A. Cano, A. A. D. C. Tolentino, A. C. V Sandoval, N. J. P. Santos, S. Daniella, M. S. Satrain, K. K. R. Sulita, J. L. Tan, and T. L. D. Tugonon, "Oil as an Alternative Clearing Agent to Xylene in Histological Staining Process: A Systematic Review," Egyptian Journal of Histology **48**(2), 397–411 (2025).

Machine Learning for Complex Physical Systems: Data-Driven Modeling of Emergent Behavior

K. EL MAJDOULI[1], M. CHAFI[1]

1 Laboratory of Condensed Matter Physics, Faculty of Sciences Ben M'sik, University Hassan II Casablanca Morocco

Hassan II University of Casablanca, Higher School of Technology of Casablanca (ESTC), Process Engineering Department, Laboratory of Process, Mechanics, Materials and Industrial Engineering (LPMMGI), Casablanca, Morocco.

E-mail: khaoula.elmajdouli-etu@etu.univh2c.ma

Introduction

In complex physical systems there are non-linear interactions between the microscopic structure and the macroscopic behavior. These systems often contain high-dimensional parameter spaces, emergent phenomena, and strong dependencies between physical variables.Traditional computational approaches such as Density Functional Theory (DFT) provide accurate predictions but may require significant computational resources for large-scale material screening. Recent developments in Machine Learning (ML) and Artificial Intelligence (AI) offer powerful alternatives for mining hidden patterns in physical data and for speeding up predictive modelling in physics and material science.

This work explores a data-driven framework for modeling complex material systems using machine learning algorithms, with hydrogen storage materials serving as a representative case study.

Scientific Context

Complex Systems Characteristics

•Nonlinear interactions

•Emergent behavior

•Multi-scale dependencies

•High-dimensional parameter spaces

•Sensitivity to structural changes

Why Machine Learning?

Machine learning enables:

•Fast prediction of material properties

•Discovery of hidden structure–property relationships

•Reduced computational cost

•Efficient exploration of large datasets

Methodology

1 Dataset

- DFT-based materials databases.
- Experimental literature datasets.

2 Feature Engineering

More than 50 descriptors were collected:

Structural Features

BET surface area , Pore volume , LCD/PLD descriptors

Elemental Features

•Electronegativity

Valence electron concentration (VEC) , Atomic radius mismatch

Operational Features

Temperature , Pressure

3 Machine Learning Models

Three supervised learning algorithms were implemented:

•Random Forest (RF)

•Support Vector Regression (SVR)

•XGBoost (XGB)

Training Protocol

•80/20 train-test split

•5-fold cross-validation

•Bayesian hyperparameter optimization

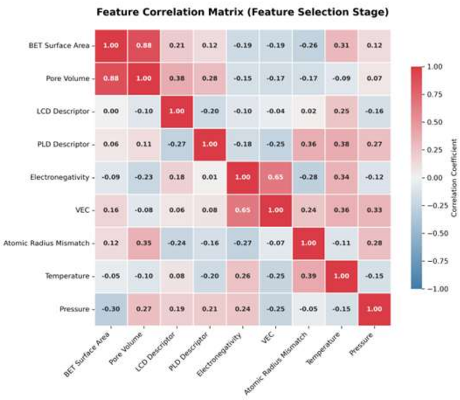

Results

Performance (Gravimetric Capacity):

Model	R^2	MAE	RMSE	MAPE
RF	0.941	0.28	0.42	4.1
SVR	0.928	0.32	0.48	4.8
XGBoost	0.952	0.25	0.38	3.7
Ensembl	0.958	0.23	0.35	3.4

Adsorption Energy:

MAE 0.28–0.42 kJ/mol.

Speedup:

<1 ms/inference, screens 10^6 candidates.

Top Features:

BET area (28.4%), pore volume (19.7%), pressure (14.2%).

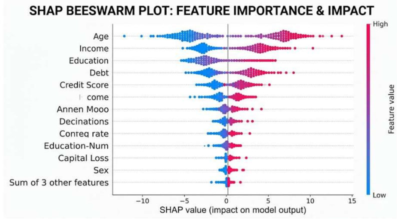

Discussion

The results demonstrate that machine learning can effectively capture nonlinear relationships between material structure and hydrogen storage performance.

Physical Insights

•In MOFs, porosity dominates adsorption behavior

•In metal hydrides, electronic descriptors such as VEC strongly influence reversibility

The obtained performance is consistent with recent state-of-the-art studies in materials informatics.

Conclusion

This work demonstrates the immense potential of machine learning for modeling complex physical systems and accelerating the discovery of novel hydrogen storage materials.By implementing the proposed data-driven framework, researchers can achieve high predictive accuracy while drastically reducing traditional computational costs. Ultimately, this approach enables the rapid exploration of vast material design spaces, establishing AI-driven methodologies as a highly promising pathway toward the development of next-generation sustainable energy technologies.

Future Work

•Graph Neural Networks (GNNs)

•Active learning strategies

•Multi-objective optimization

•Hybrid experimental-computational pipelines

•Integration with DFT simulations

KeyWords

Machine Learning, Complex Systems, Hydrogen Storage, XGBoost, Materials Informatics, Computational Physics, AI for Energy, Data-Driven Discovery

References

1. R. Kumar, A. Sharma, and L. Zhang, "Accelerating Hydrogen Storage Material Discovery via Machine Learning: From Descriptors to High-Throughput Screening," *Journal of Materials Chemistry A*, 2024, 12, 4512–4528.

2. J. Wang, Y. Liu, and M. Chen, "Predicting Hydrogen Adsorption Capacity in Metal-Organic Frameworks Using Gradient Boosted Trees and Feature Engineering," *Computational Materials Science*, 2025, 234, 112780.

3. S. Patel, H. Kim, and T. Nguyen, "Multi-scale Modeling of Complex Physical Systems: Integrating Density Functional Theory with Ensemble Machine Learning Frameworks," *Physical Review Materials*, 2025, 9, 034005.

4. L. Müller, O. Schmidt, and J. Petit, "Data-Driven Informatics for Next-Generation Sustainable Energy Technologies: A Review of AI in Hydrogen Storage," *Advanced Energy Materials*, 2026, 16, 2500124.

A Tunable Electrowetting Microlens on an Optical Fiber Tip

R. Eskandani [1], **M. I. Zibaii** [1,2], **F. Behdadkia** [3], **and H. Latifi** [1,3]

[1] *Laser and Plasma Research Institute, Shahid Beheshti University, Tehran, Iran*
[2] *Institute for Cognitive and Brain Sciences, Shahid Beheshti University, Tehran, Iran*
[3] *Physics Department, Shahid Beheshti University, Tehran, Iran*

Optical systems capable of dynamically focusing and steering the beam of light often rely on bulky or mechanically complex components, limiting their integration into miniaturized devices for application in optogenetics, biomedical imaging and optical sensing [1, 2]. This work proposes an electrowetting liquid microlens integrated on the tip of an optical fiber, which enables compact light delivery with electrically controlled focusing and beam steering. A multiphysics simulation framework is developed to evaluate the proposed system prior to experimental realization while considering microfabrication uncertainties and dimensional variations. The framework combines fluid dynamics, light wave propagation, and thermal analysis to investigate voltage-controlled lens deformation, beam focusing, steering, and temperature variations under optical illumination. Machine-learning models are further explored to accelerate prediction of optical and thermal responses across different design parameters. The simulation results suggest the feasibility of the proposed system and provide design guidelines for fabrication optimization, reducing development iterations and supporting future experimental implementation.

[1] M. G. Craske, M. M. Herzallah, R. Nusslock, V. Patel, Nat. Ment. Health **1**, 12 (2023).
[2] F. Akbari et al., Eur. Conf. Lasers Electro-Optics, Optica Publishing Group, (2019).

P14

Title **Multisolitons-like patterns in a one-dimensional MARCKS protein cyclic model**

Chenceline Fouedji[1], **Chenceline Fouedji**[1], Armand Sylvin Etémé[1], Conrad Bertrand Tabi[2], Henri Paul Ekobena Fouda1

[1] Laboratory of Biophysics, Department of Physics, Faculty of Science, University of Yaoundé I, P.O. Box 812, Yaoundé, Cameroon

[2] Botswana International University of Science and Technology, P/Bag 16, Palapye, Botswana a *Laboratory of Biophysics, Department of Physics, Faculty of Science, University of Yaoundé I, P.O. Box 812, Yaoundé, Cameroon*

Abstract We analytically investigate the conditions for the wave instability in a reaction-diffusion system describing the nonlinear dynamics of the myristoylated alanine-rich C kinase substrate (MARCKS) between cytosol and cytoplasmic membrane [1]. Taking into account the effect of spatial inhomogeneous diffusion coefficients, and by applying the discrete multiple scale expansion method, we show that the nonlinear generic model can be transformed into a one-dimensional discrete nonlinear Schrödinger equation [2]. We perform a linear stability analysis on the plane wave solutions to derive the criterion of the modulational instability (MI) phenomenon. This analysis reveals that the critical amplitude of the plane wave is highly influenced by the phosphorylation rate and weakly influenced by the inhomogeneous diffusion coefficients. The exact analytical solutions show that the system exhibits traveling waves and periodic array of patterns. The results seem to indicate the features of synchronization in the collective dynamics. In homogenous state, we obtained a spatial pattern of horizontal stripes. By considering the spatial inhomogeneity effect, we obtain a spatial pattern of oblique stripes. We also notice that an increase in wavenumber induces the increase in the number of stripes in the model.

References

[1] M. El Amri, U. Fitzgerald, G. Schlosser, MARCKS and MARCKS-like proteins in development and regeneration. J. Biomed. Sci. 25, 43 (2018)

[2] S. Alonso, M. Bär, Phase separation and biostability in a three-dimensional model for protein domain formation at bio membranes. Phys. Biol. **7**, 046012 (2010)

P15

Collective pattern formation in pulse-driven swarmalators

Samali Ghosh[1], **Kevin O'Keeffe**[2], **Gourab Kumar Sar**[3], **and Dibakar Ghosh**[1]

[1] *Physics and Applied Mathematics Unit, Indian Statistical Institute, 203, B.T. Road, Kolkata 700108, India*

[2] *Starling Research Institute, Seattle, Washington, USA*

[3] *Complexity Science Group, Department of Physics and Astronomy, University of Calgary, Calgary, AB, Canada*

The physics of complex systems seeks to unravel the fundamental mechanisms by which collective, self-organizing behaviors emerge from the interactions among various individual components. In nature, these collective patterns often involve two intertwined processes: spatial movement and rhythmic activity in time. Swarmalators [1] describe a distinct class of system that couples spatial dynamics with internal rhythmic behavior. These are the kind of self-propelled particles whose spatial motion emerges from the collective aggregation of the swarming agents, while their internal dynamics are characterized by intrinsic oscillatory behavior. The model captures a diverse range of collective patterns that closely mirror real-world phenomena. To date, the Kuramoto model remains the predominant framework for describing each oscillator's intrinsic phase dynamics. Several well-studied biological phenomena, such as flashing fireflies, Japanese tree frogs croaking, neuronal spike trains, rhythmic clapping in crowds, and technical systems such as communications in wireless sensor networks or drone swarms, involve pulsatile rather than continuous interactions. In 1967, Winfree proposed a model by introducing globally coupled oscillators where agents communicate through signal emission and response [2]. The system exhibits a remarkable transition from asynchrony to synchrony, closely resembling the phase transition in statistical mechanics. Therefore, plugging the Winfree system into generic swarmalator dynamics can provide a more comprehensive and biologically relevant paradigm for modeling their collective behavior. In this work, we have studied a simple 1D swarmalator ring model where interactions occur through brief, discrete pulses. We have checked the system for both identical [3] and non-identical [4] perspectives. This general interaction approach reveals rich collective patterns (including similar and novel states), and we successfully analyze the stability thresholds for the states.

[1] O'Keeffe, K. P., Hong, H., & Strogatz, S. H. (2017). Oscillators that sync and swarm. Nature communications, 8(1), 1504.

[2] Ariaratnam, J. T., & Strogatz, S. H. (2001). Phase diagram for the Winfree model of coupled nonlinear oscillators. Physical Review Letters, 86(19), 4278.

[3] Ghosh, S., O'Keeffe, K., Sar, G. K., & Ghosh, D. (2025). Dynamics of pulsating swarmalators on a ring. Physical Review E, 112(5), 054217.

[4] Ghosh, S., O'Keeffe, K., & Ghosh, D. (2026). Emergent dynamics in heterogeneous pulsatile swarmalators. Chaos: An Interdisciplinary Journal of Nonlinear Science, 36(3).

P16

Extreme events in moist stratified turbulence

Giordano, J.B.[1] **and Mininni, P.D.**[2]

[1] *Universidad de Buenos aires, Facultad de Ciencias Exactas y Naturales, Departamento de Fisica, Ciudad Universitaria, Buenos Aires 1428, Argentina.*

[2] *Universidad de Buenos aires, Facultad de Ciencias Exactas y Naturales, Departamento de Fisica, CONICET-UBA INFINA, Ciudad Universitaria, Buenos Aires 1428, Argentina.*

We study numerically the occurrence of extreme events in stably stratified turbulence with moisture, under conditions relevant to the Earth's atmosphere. Extreme events play a crucial role in weather and climate, and their origin is not fully understood. They are common in many nonlinear systems, and in turbulence in particular. However, their dynamics in the presence of moisture has not been studied before. Previous studies in dry stratified flows have shown the presence of extreme values in the velocity and temperature fluctuations, localized in space and in time [1, 2], but with properties that are different from extreme events in isotropic and homogeneous turbulence. In particular, in stratified flows extreme events develop in large-scale patches, creating localized regions of strong turbulence and energy dissipation. This phenomenon is observed in geophysical flows, such as in clear-air turbulence in the atmosphere [3], or in oceanic flows where energy dissipation was shown to be intermittent and sporadic in space [6].

The lack of studies including the effect of moisture in stratified turbulence is the main motivation for this work, as moisture plays a central role in cloud formation and droplet size distributions [4, 5]. To address this, a simple moisture model based on the Boussinesq approximation [7] is numerically implemented. This model allows us to compute, at each fluid parcel, the fraction of water in liquid and vapor phases, as well as the heat released during phase transitions. The simulations were performed using the GHOST code [8]. We show how intermittency and the occurrence of extreme events is affected by moisture, exploring parameter space for different levels of the background atmospheric stratification, and for the saturation of the atmosphere. In the future we plan to connect these results with simple nonlinear dynamical models for the three relevant variables in the system: the water content of each fluid element, the buoyancy force acting on each fluid element, and the vertical velocity of each parcel

References

[1] F. Feraco, R. Marino, A. Pumir, L. Primavera, P.D. Mininni, A. Pouquet, D. Rosenberg, EPL **123**, 44002 (2018).

[2] R. Marino, F. Feraco, L. Primavera, A. Pumir, A. Pouquet, D. Rosenberg, P.D. Mininni, Phys. Rev. Fluids **7**, 033801 (2022)

[3] P. Rodriguez Imazio, A. Dörnbrack, R. Delgado Urzua, N. Rivaben, A. Godoy, J. Geophys. Res. Atmospheres **127**, e2021JD035908 (2022).

[4] I. Saito, T. Gotoh, New J. Phys. **20**, 023001 (2018)

[5] E. Bodenschatz, S.P. Malinowski, R.A. Shaw, F. Stratmann, Science **332**, 970 (2010)

[6] P. Pearson, B. Fox-Kemper, Phys. Rev. Lett. **120**, 094501 (2018).

[7] D.H. Marsico, L.M. Smith, S.N. Stechmnn, J. Atmosph. Sc. **76**, 3569 (2019).

[8] P.D. Mininni, D. Rosenberg, R. Reddy, A. Pouquet, Parallel Comp **37**, 316 (2011).

Lifetime of a Forager : Effect of Environment and Strategies

Sanchari Goswami [1]

[1] *Vidyasagar College, Kolkata*

Foraging is a habitual tendency for all living organisms, where the forager is in search of a resource. In most cases, a forager moves from one place to another in search of the resource, the most common and essential of which is perhaps, food. From the ancient times, human beings, all initially located in Africa, started spreading to other places in searchof resources, thereby populating the rest of the world [1].

In this work, we study foragers from two perspectives. In the first, we study the fate of a forager which searches for food, at the same time performing a random walk on lattices. The forager consumes the available food on a site it visits and leaves it depleted. The starvation time of the forager is S, which means it can survive up to S steps without food. We introduce the concept of intermittent rest in the dynamics. This allows the forager to take rest with probability p upon consumption of food. It has been observed that the parameter p significantly alters the lifetime of the forager, showing that the intermittent rest can be beneficial for the forager for chosen parameter values. Various other quantities have been studied in this context that those reveal interesting scaling behavior with p. Departure from usual diffusive behavior for $0.5 < \mathrm{p} < 1$ has also been observed. In addition to numerical simulations, the problem has also been studied analytically in one dimension and the results up to $\mathrm{p} < 0.5$ agree with the numerical ones.

In the second, we tried to address the question whether it is necessary for a living organism to always eat whenever it comes across some food in a fear, that, later it may not find any. In that approach, we consider partial consumption of food in presence of a threshold energy of a forager. The threshold limits the consumption of food in such a way that, whenever the forager energy is above the threshold, it will not consume any food. In some earlier works, the options of taking food whenever it encounters a site containing food [2] or only when its energy falls below a certain threshold value [3] have been considered. The forager considered here has starvation time S. At the same time, it consumes food only when its energy falls below a threshold k. A limiting case is a normal forager with $k = S - 1$. In contrast, forager with $k = 0$ is a forager which takes food after complete exhaustion of energy. The add-on here is partial consumption of food. Thus, a site containing food may not always be fully depleted and therefore, there is a chance of slow growth of the desert, which in turn helps in increasing the lifetime of the forager. It has been observed that as the threshold fraction k/S increases from a very low value, the lifetime increases abruptly at the beginning, then reaches a high value at some transition threshold k^*/S and never decreases thereafter, although the growth rate becomes low. The transition threshold $k^* \sim \sqrt{S}$. The lifetime τ when considered with variation of S, keeping k/S a parameter, shows a power law behavior as a$\tau \sim S^{\beta}$. For $\frac{k}{S} = 0,\ \beta = 4/3$. The exponent β then jumps above 2 and decreases gradually to 1.84. Number of revisitations to a site, food statistics are the other important quantities are also studied and show some interesting scaling behavior.

[1] O. Stephen, Philos. Trans. R. Soc. B 367, 770 (2012).
[2] O. Benichou and S. Redner, Phys. Rev. Lett. 113, 238101(2014).
[3] O. Benichou, U. Bhat, P. L. Krapivsky and S. Redner, Phys. Rev. E 97, 022110 (2018).

P18

Assessment of Pollution Load Index of Soil and Dust Particles at Ghana Kpone Landfill Site and Health Risks to Waste Scavengers

Aretha Makafui Nuviadenu[1], Owiredu Gyampo[1,2], Sampson Atiemo[4], Christian Nuviadenu[1,2], Hyacinthe Ahiamadjie[1,2], Samuel Amiteye[1,3], Karikari Williams[4]

[1]School of Nuclear and Allied Sciences (SNAS), College of Basic and Applied Sciences (CBAS), University of Ghana, Atomic Energy-Accra, Ghana.
[2]National Nuclear Research Institute, Ghana Atomic Energy Commission, Accra Ghana
[3]Biotechnology and Nuclear Agriculture Research Institute (BNARI), Ghana Atomic Energy Commission (GAEC), Accra, Ghana.
[4]Mountain Research Institute, P.O. Box KF1424, Koforidua

The high consumption rate of goods and products today has directly impacted the volumes of waste generated. In developing countries, mixed waste volumes usually choke the landfills with waste scavengers selecting valuables (recyclables) as secondary raw materials to feed the recycling industries. In Ghana, these scavengers (mostly informal) lack the required tools and equipment to ensure their safety at the landfill sites considering the harmful nature of the unsegregated Municipal Solid Waste. At the Kpone Landfill site in Ghana, the study assessed the environmental pollutants in soil and resuspended dust using the X-ray Fluorescence technique. Eight heavy metals; V, Cr, Ni, Cu, Zn, Cd, Hg, and Pb were identified and measured in soil and dust samples taken from ten locations within the study area. Cu, Zn, and Pb recorded the highest concentrations as; 334 mg/kg, 36585 mg/kg, 4808 mg/kg respectively, exceeding their respective New Dutch List acceptable limits. Contamination factors based on elemental concentrations, as well as the degree of contamination calculated for each sampling location, revealed that locations 4, 5, 6, and 7 were significantly contaminated. Health hazard index for both non-carcinogenic and carcinogenic health risks for ingestion, dermal, and inhalation exposure pathways; forecasted locations 4, 5, 6, and 7 as significant health risks for waste pickers who work in these areas.

P19

Uniform Liquid Crystalline 2D Hybrid Films for Humidity Sensing

Sara Gyozalyan [1], **Lilit Avanesyan** [1], **Marina Zezhu**[1], **Alexey Vasil'ev**[1], **Hermine Gharagulyan**[1,2]

[1] *Liquid Crystalline Nanosystems Research Group, A.B. Nalbandyan Institute of Chemical Physics NAS RA, Yerevan, 0014, Republic of Armenia*

[2] *Institute of Physics, Yerevan State University, Yerevan, 0025, Republic of Armenia*

Two-dimensional (2D) hybrid nanocomposites have recently gained considerable attention as advanced materials for environmental sensing, due to the cooperative interactions between their individual components. Such systems can surpass the intrinsic limitations of single-component materials by providing improved sensitivity, selectivity, and rapid response characteristics. In this work, we present a hydrothermally synthesized tungsten disulfide/reduced graphene oxide hybrid, stabilized with polyvinylpyrrolidone (PVP), forming a 1T-WS_2/PVP/rGO nanocomposite. Notably, the material exhibits liquid crystalline behavior, which enables controlled self-organization into highly uniform thin films which is an essential feature for reliable sensing applications. A detailed opto-structural characterization of the composite is performed to elucidate its morphology and functional properties. The humidity sensing performance is evaluated in terms of response dynamics, including response and recovery times. Furthermore, the liquid crystalline ordering facilitates uniform alignment, which contributes to improved charge transport and sensing efficiency. Overall, this study highlights a versatile platform for high-performance humidity sensing, with potential applications in wearable devices and environmental monitoring systems. [1].

This work was supported by No. 24LCG-2F027 grant of RA MESCS Higher Education and Science Committee.

[1] A. Vasil'ev, M. Zhezhu, S. Gyozalyan, L. Avanesyan, Y. Grigoryan, A.A. Kuzanyan, A. A. Hovhannisyan, Mohamed Aly Saad Aly, D.A. Ghazaryan, H. Gharagulyan, J. Sci. Adv. Mat. Dev., **11**, 1, 01115 (2026).

P20

Van der Waals technologies: designing distributed Bragg reflectors and dichroic beam splitters using vdW muscovite

M. H. Hayrapetyan[1], M. L. Sargsyan[1], D. A. Karakhanyan[1], A. P. Khachatryan[1] , M. A. Levonyan[1] , A. V. Margaryan[1] , M. Šiškins[2,3] , K. S. Novoselov[2,4] & D. A. Ghazaryan[1]

[1]*Laboratory of Advanced Functional Materials, Yerevan State University, Yerevan, 0025, Republic of Armenia*

[2]*Institute for Functional Intelligent Materials, National University of Singapore, Singapore, 117575, Republic of Singapore*

[3]*School of Physics and Astronomy, University of Southampton, Highfield, Southampton, SO17 1BJ, United Kingdom*

[4]*Department of Materials Science and Engineering, National University of Singapore, Singapore, 117575, Republic of Singapore*

Van der Waals (vdW) crystals offer unique opportunities for modern nanophotonic applications owing to their layered structure and tunable optical properties. While many vdW crystals exhibit pronounced anisotropy and relatively high refractive indices, comparatively little attention has been given to low-index, weakly anisotropic vdW dielectrics. In this context, muscovite (or mica) represents an intriguing yet underexplored material platform, combining atomically flat surfaces with low optical losses and weak in-plane anisotropy. When paired with a high refractive index vdW crystal into a heterostructure, its low index enables large index-contrasts, facilitating tailored optical response in ultrathin multilayer architectures. These characteristics make it particularly attractive for realizing broadband photonic components with reduced scattering and absorption losses.

In this work, we present a comprehensive determination of broadband dielectric permittivity tensor of vdW muscovite across the ultraviolet (UV) to near-infrared (NIR) spectral region. By resolving its anisotropic optical response, we extract accurate tensor components and show that muscovite exhibits consistently low refractive indices, negligible extinction and weak in-plane anisotropy, enabling its effective description as a uniaxial dielectric in the thin-film limit. Leveraging the large refractive index contrast between muscovite and high-index MoS_2, we design ultrathin heterostructures based on strong interference effects in lossless spectral regions. This enables the realization of few-layer distributed Bragg reflectors (DBRs) and dichroic beam splitters (DBSs) with high reflectivity, broad spectral selectivity, and robust performance in NIR, all within sub-micron thicknesses. Overall, our results highlight the critical role of low-index, lossless vdW crystals in high-contrast optical design and establish muscovite as a highly promising platform for ultracompact, broadband, all-vdW nanophotonic devices.

P21

Towards Quantum Imaging with Undetected Light

Daliborka Hranjec[1,2]

[1]*Institute of Physics Belgrade*
[2]*Faculty of Physics, University of Belgrade*

Many molecules exhibit strong absorption features in the mid-infrared spectral range, while cameras operating in this range are expensive, prone to noise, and offer lower resolution than conventional visible-range cameras. Such challenges can be addressed by exploiting quantum correlation between photon pairs, allowing an object to be probed with a photon of one wavelength, while its correlated partner of another wavelength is detected.

This approach, known as quantum imaging with undetected light (QIUL), decouples the illumination and detection wavelengths, enabling imaging in spectral regions where suitable detectors are unavailable or perform poorly at the sample probing wavelength, giving it advantage over conventional imaging methods.

In this work we build an interferometric QIUL setup (following [1]) and use computational modeling (following [2]) to power its optimization. We address the problem of image post-processing using deconvolution algorithms and propose using convolutional neural networks for denoising images. As our first milestone, we demonstrate interference between photons generated in the experimental setup.

[1] M. Gilaberte Basset, *Resolution Limits of Quantum Imaging with Undetected Light and Optimization Towards Application*, PhD Thesis (2024).

[2] F. Riexinger, *Simulation Methods for Spontaneous Parametric Down-Conversion and Quantum-Sensing Systems with Undetected Light*, PhD Thesis (2023).

The 10th International Conference on Mechanics and Energy

December 25-27, 2025, Hammamet, TUNISIA

2025

P22

Green synthesis of silver nanoparticles from Carpobrotus edulis for the photothermal assay of the tumor biomarker CA 19-9

Chaima JBIRA[1], Rochdi BAATI[1],

[1] Laboratory of Laboratory of Energy and Materials, Higher School of Sciences and Technology of Hammam Sousse, University of Sousse, TUNISIA

Introduction

Early and sensitive detection of tumor biomarkers is crucial for improving cancer diagnosis and follow-up, especially for pancreatic cancer where CA 19-9 is widely used.• Silver nanoparticles (AgNPs) exhibit strong plasmonic/photothermal properties enabling easy readout.• Green synthesis using plant extracts provides an eco-friendly, low-cost route.

Objectives

1- Synthesize AgNPs via Carpobrotus edulis aqueous extract.
2. Compare heating and microwave routes.
3. Characterize AgNPs (UV–Vis, FTIR, DLS, zeta, SEM).4. Develop a photothermal assay for CA 19-9 without antibodies.

Green synthesis principle

In green synthesis, the Carpobrotus edulis aqueous extract provides natural phytochemicals (polyphenols, flavonoids, sugars, proteins) that act as both reducing and capping agents. When mixed with $AgNO_3$ and heated or microwave-irradiated, these biomolecules donate electrons to reduce Ag^+ into Ag^0. The resulting Ag^0 atoms undergo nucleation and growth to form AgNPs, evidenced by a light-orange to brown color change and a surface plasmon band in UV–Vis spectra. Remaining plant compounds adsorb on the nanoparticle surface (–OH, –COOH, $–NH_2$ groups), stabilizing the AgNPs without toxic chemicals.

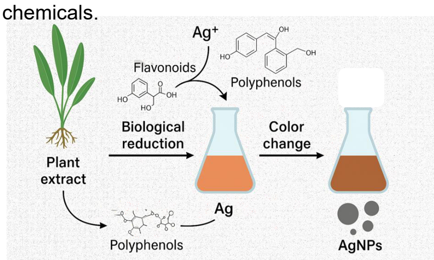

Materials & Methods

Plant extract preparation:• Wash and dry plant parts (stem, leaves, flowers).
• 300 g plant + 1 L distilled water; boil 100°C for 1 h with magnetic stirring
• Filter or centrifuge (4000 rpm, 10 min) → clear extract.AgNP synthesis ($AgNO_3$:extract = 40:60):• $AgNO_3$ solutions 1–5 mM (100 mL).• Heating: 60/80/100°C; 1–3 h; [$AgNO_3$] 1–4 mM.• Microwave: 200/400/600 W; 3–10 min; [$AgNO_3$] 1–4 mM.
Characterization: UV–Vis, FTIR, DLS, zeta potential, SEM, photothermal tests.

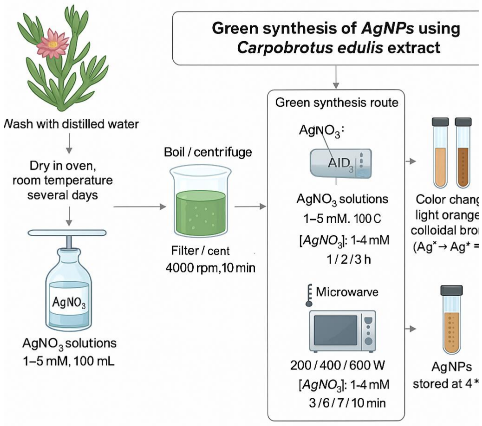

Fig 1. synthesis flowchart

Characterization results

UV–Vis: plasmon band confirms AgNPs; decrease of flavonoid bands (270–283 nm) indicates oxidation during Ag^+ reduction
• FTIR: shifts highlight phenolic/amine groups involved in reduction/capping.
• SEM shows agglomerated AgNPs.
• DLS: 400–700 nm hydrodynamic size.
• Zeta potential ≈ −17 mV → limited stability.

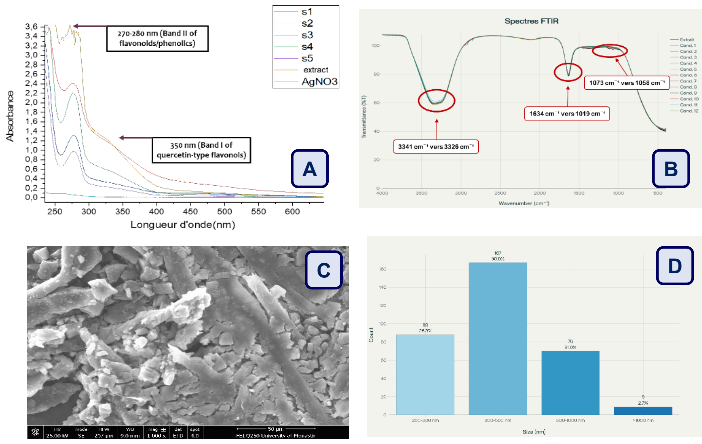

Fig 2. A:UV–Vis, B:FTIR, C:SEM, D: DLS

Photothermal assay of CA 19-9

The mixture of CA 19-9 with AgNPs without antibodies shows a significantly enhanced photothermal signal compared to individual components (0.09-0.79) (figure 3), confirming direct interaction between the AgNPs surface and the biomarker. This synergy validates the innovative hypothesis for CA 19-9 detection.(figure 4) .

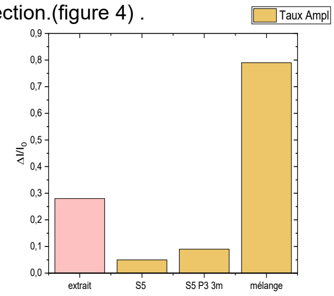

Fig 3. photothermal signal compared to individual components

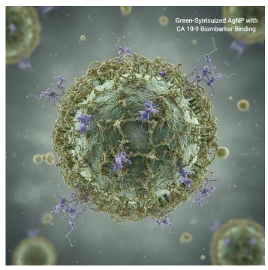

Fig 4 interaction between the AgNPs surface and the biomarker

Conclusion

Green synthesis of AgNPs using Carpobrotus edulis is successful.
• Microwave route enables rapid and efficient production.
• Optimized AgNPs provide a simple, low-cost photothermal assay for CA 19-9 without antibodies.
• Promising platform for early pancreatic cancer screening

P23

Chaotic Optoelectronic Oscillator for Secure Biomedical Image Encryption Using Neural Network Modeling

Gabin Kitio Jeatsa[1]
[1]Department of Electrical Engineering, University of Dschang, Cameroon

Abstract

In this work, we propose a nonlinear chaotic optoelectronic oscillator for secure biomedical image encryption. The system is based on a high-dimensional nonlinear dynamical model capable of generating complex chaotic signals with high sensitivity to initial conditions, which is a key property for cryptographic applications.The dynamical behavior of the proposed oscillator is investigated through phase portraits, bifurcation diagrams, and Lyapunov exponents, confirming the presence of chaotic regimes. The generated chaotic sequences are then employed to design an efficient encryption scheme for biomedical images, ensuring strong security features such as low pixel correlation, high entropy, and resistance to noise and data loss. Furthermore, a neural network based on radial basis functions is implemented to approximate and predict the chaotic dynamics of the system. The model is trained using simulated data and optimized using a least squares approach, providing accurate reconstruction of the system trajectories. The obtained results demonstrate that the combination of nonlinear dynamics, optoelectronic implementation, and machine learning offers a robust framework for secure biomedical data processing. This work highlights the relevance of complex systems in modern cryptographic applications.

References

[1] L. M. Pecora and T. L. Carroll, *Synchronization in chaotic systems*, Phys. Rev. Lett. 64, 821–824 (1990).
[2] G. Chen and X. Dong, *From Chaos to Order: Methodologies, Perspectives and Applications*, World Scientific (1998).
[3] S. Haykin, *Neural Networks and Learning Machines*, 3rd ed., Prentice Hall (2009).

P24

Seeking Criticality In Real Brain Networks

Mina Khorrambakht and Saman Moghimi-Araghi

Physics department, Sharif University of Technology, P.O. Box 11155-9161, Tehran, Iran

The **critical brain hypothesis** proposes that the brain operates near a critical point, where certain response functions diverge at a phase transition. Classically, reaching such a point requires precisely tuning an external control parameter (e.g., temperature) — raising the question of:

What could tune the brain to criticality or whether fine-tuning is even necessary?

Here, we explore the possibility that quenched structural heterogeneity in real neural networks relaxes this requirement: rather than a single sharp phase transition, disordered network topology may give rise to a **Griffiths phase** — *an extended region of parameter space exhibiting critical-like dynamics without the need for precise tuning* —. We investigate this framework using an excitable dynamics model on empirical connectome networks.

P25

Hydrological Connectivity-Induced Bifurcations in a Shallow Wetland Lake: The Case of Wolong Lake

<u>Lu Xinyi</u> [1] , Teh Su Yean [2]

[1] *School of Science/Aesthetic Education Center, Shenyang Institute of Engineering, 110136 Shenyang, Liaoning, China*

[2] *School of Mathematical Sciences, Universiti Sains Malaysia, 11800 USM, Pulau Pinang, Malaysia*

Regime shifts in shallow lake ecosystems are widely recognized as a central problem in complex systems and environmental modelling. Wolong Lake, a typical shallow wetland lake in northeast China, is characterized by pronounced spatial heterogeneity, with a relatively pristine northern basin and a nutrient-enriched southern basin separated by a natural topographic sill. This configuration is considered an ideal natural setting in which the influence of hydrological connectivity on nonlinear ecological transitions can be investigated.

In this study, a bifurcation-based modelling framework is developed to examine the role of hydrological connectivity in driving regime shifts between alternative stable states. Nutrient dynamics, external loading, and inter-basin water exchange are incorporated into the model, and key feedback mechanisms between hydrodynamics and ecological processes are captured. Through numerical simulations, it is shown that variations in connectivity strength can induce critical transitions, hysteresis, and tipping points in water quality states. It is further demonstrated that hydrological connectivity can exert both stabilizing and destabilizing effects depending on nutrient conditions, highlighting its dual role in complex lake systems. These findings provide insight into the mechanisms underlying abrupt ecological changes, and potential implications for wetland lake management and restoration are suggested.

This work contributes to the broader understanding of complex systems, in which spatial heterogeneity, nonlinear dynamics, and environmental forcing are coupled, and relevance to computational modelling in interdisciplinary research across the physical and life sciences is emphasized.

P26

Geometric Defects Control the Effective Diffusion Exponent of Active Swimmers

Yhony M. Arce[1]**; William Oropesa**[1]**; André P. Vieira**[3]**; Hartmut Löwen**[4]**; Danilo B. Liarte.**[1,2]

[1] *Institute of Theoretical Physics, São Paulo State University, São Paulo, Brazil*
[2] *ICTP South American Institute for Fundamental Research, São Paulo, Brazil*
[3] *Institute of Physics, University of São Paulo, São Paulo, Brazil*
[4] *Heinrich-Heine Universität Düsseldorf, Düsseldorf, Germany*

Self-propelled particles transport very differently depending on the geometry of the medium they move through, from cells swimming through tissue to synthetic microswimmers in porous materials [1]. We study a minimal model of an active particle whose swimming direction couples to the layer orientation of a smectic liquid crystal, a layered material that can host ordered defects known as focal conic domains. In a defect-free texture, and even near an isolated defect, the particle's diffusion grows quadratically with its swimming speed — the ballistic scaling expected for a free swimmer. In a hexagonal lattice of these defects, however, that growth slows continuously toward ordinary linear scaling as the coupling between swimming direction and layer orientation strengthens, reflecting a competition between the particle's own persistence and repeated redirection by the defect lattice. A geometric texture, we show, can control active transport as strongly as self-propulsion itself.

[1] C. Bechinger, R. di Leonardo, H. Löwen, C. Reichhardt, G. Volpe and G. Volpe, *Rev. of Mod. Phys.* **88**, 045006 (2016).
[2] C. Ferreiro-Córdova, J. Toner, H. Löwen and H. H. Wensink, *Phys. Rev. E* **97**, 062606 (2018).

P27

SYNTHESIS of Nd:YAG NANOPARTICLES by THE SOL-GEL METHOD: THERMAL ANALYSIS and PHOTOLUMINESCENCE PROPERTIES

***T.N. Mammadova*, T.G. Naghiyev**

Azerbaijan State University of Economics (UNEC), Baku, Azerbaijan

Yttrium aluminum garnet ($Y_3Al_5O_{12}$, YAG) has long been regarded as one of the most reliable host matrices for rare-earth luminescence, largely because of its high thermal and chemical stability, combined with an exceptionally broad optical transparency range. When the material is prepared at the nanoscale, these bulk advantages are retained while new possibilities emerge: a greatly enlarged surface area, improved sinterability, and the potential for dispersion in colloidal systems. Doping the garnet lattice with Nd^{3+} ions introduces efficient near-infrared emission, making the resulting nanoparticles relevant to both solid-state laser technology and emerging biomedical imaging applications.

In this work, Nd^{3+} doped YAG nanoparticles were prepared by a citrate sol-gel route. Stoichiometric amounts of the corresponding nitrate and oxide precursors were dissolved in deionized water with citric acid as a chelating agent, and the pH was adjusted to 7 using ammonia solution. The resulting sol was slowly dried at 90 °C to produce a porous xerogel, which was then calcined in air over the temperature range 800-1000 °C. Nd^{3+} concentrations of 5 mol% were investigated in order to identify the composition that yields the strongest photoluminescence response[1].

Thermal behavior of the xerogel was studied by simultaneous TGA/DSC measurements up to 1100°C. The thermogram revealed three well-separated events: water evaporation below 200°C, an intense exothermic combustion of the citrate network near 310 °C responsible for the largest mass loss in the run (40 wt%), and a moderate exotherm around 850 °C marking the onset of garnet crystallization. This last event produces negligible additional weight loss, confirming that it reflects a solid-state structural transformation rather than further decomposition. These data provided a clear basis for selecting the minimum calcination temperature needed to obtain a single-phase product.

Photoluminescence measurements were performed at room temperature using a 785 nm laser as the excitation source. All samples exhibited strong near-infrared emission, with the dominant peak at 1064 nm corresponding to the $^4F_{3}/_{2} \rightarrow {}^4I_{11}/_{2}$ transition of Nd^{3+}. A secondary emission band near 940 nm, arising from the $^4F_{3}/_{2} \rightarrow {}^4I_{9}/_{2}$ transition, was also clearly resolved. Among the compositions studied, the 5 mol% Nd^{3+} sample calcined at 1000 °C produced the highest emission intensity at 1064 nm, while exceeding this concentration led to a gradual decrease in output attributed to concentration quenching[2].

The results show that the citrate sol-gel method is a straightforward and effective approach for obtaining phase-pure Nd:YAG nanoparticles at moderate temperatures. The thermal analysis data proved particularly useful in guiding the choice of calcination conditions, and the photoluminescence measurements confirmed that the near-infrared emission characteristics of the synthesized powders are well suited to practical applications in laser and imaging technologies.

[1] E. De la Rosa, L.A. Díaz-Torres, P. Salas, A. Arredondo, J.A. Montoya, C. Angeles, R.A. Rodríguez, Opt. Mater. 27, 1793 (2005).

[2] M.S. Kurrey, A. Tiwari, M.S.K. Khokhar, R.S. Kher, S.J. Dhoble, J. Lumin. 164, 94 (2015).

P28

Effect of Soil and Water Conservation on Plant Diversity and Community Structure in Atsbi-Wenberta, Tigray, Ethiopia

Zufan Desta [1, 2], Emiru Birhane [3, 4, 5], Mitiku Haile [3], Dawit Gebregziabher [1]

[1]*Department of Agricultural and Resource Economics, Mekelle University, Mekelle, Tigray, Ethiopia*

[2]*Department of Natural Resource Management, Adigrat University, Adigrat, Tigray, Ethiopia*

[3]*Department of Land Resource Management and Environmental Protection, Mekelle University, Mekelle, Tigray, Ethiopia*

[4]*Faculty of Bioscience and Aquaculture, Nord University, Steinkjer, Norway.*

[5]*Department of Range and Forest Resources, Botswana University of Agriculture and Natural Resources, Gaborone, Botswana*

Abstract

Land degradation driven by soil erosion and deforestation poses a major threat to biodiversity and ecosystem services by altering plant species diversity and community composition [1, 2]. Biophysical soil and water conservation practices are widely implemented to rehabilitate degraded landscapes [3]; however, their effects on vegetation diversity and community structure in hilly sub-watersheds remain insufficiently quantified. This study evaluates the impact of integrated SWC measures on plant species composition, diversity, and regeneration in the Atsbi-Wenberta highlands of Tigray, northern Ethiopia. Vegetation and soil data were collected from treated and untreated sub-watersheds along slope gradients. Plant species diversity was assessed using standard diversity indices, and community types were identified through hierarchical clustering. Regeneration status was evaluated based on the distribution of seedlings, saplings, and mature individuals. In addition, Principal Component Analysis (PCA) was employed to examine relationships between species composition and key soil properties.

The results showed that SWC-treated sub-watersheds supported higher species richness and diversity compared to untreated areas. Woody species density was higher in conserved sites, particularly in lower-slope positions. Approximately 62.5% of woody species exhibited regeneration ranging from fair to good, indicating improved vegetation recovery under conservation management. PCA results revealed strong associations between plant community composition and soil variables, particularly organic matter, soil moisture content, and pH. These findings demonstrate that SWC practices significantly enhance plant diversity, regeneration, and community structure in degraded hilly landscapes. The study highlights the importance of integrating conservation interventions with landscape-level considerations to promote sustainable ecosystem restoration. Scaling up SWC measures and implementing long-term monitoring are recommended to sustain ecological benefits and support biodiversity conservation in dryland regions.

Keywords: Ecology; dryland agroecosystems; plant community dynamics; soil conservation practices; species richness; vegetation composition.

Reference

[1] B. Dhehibi, C. Zucca, A. Frija, and S. N. Kassam. New Medit 17, 15-28 (2018).

[2] R. Pandit, J. Parrota, Y. Anker, E. Coudel, L. Montanarella, R. Scholes, and A. Brainich. 435-528 (2018)

[3] A. Tilahun, and F. Belay. Journal of Degraded and Mining Lands Management 6, 1653 (2019).

P29

Architecture of Coexistence: Topological Constraints of Biodiversity in Competitive Ecosystems

G.Montagnani[1]

[1]*Department of Physics and Astronomy, University of Bologna, Bologna, Italy*

Understanding transitions between stability regimes is crucial for predicting the dynamical evolution and potential fragility of complex ecosystems. However, the influence of network structure on the organization of equilibrium states (static attractors) is still not fully understood.

Starting from the seminal work of Robert May [1], most foundational studies in theoretical ecology relied on unstructured, random interaction networks, in contrast to empirical observations, which show substantial structure [2]. We therefore investigate how structured interaction networks modify the landscape of equilibrium states.

We study how two structural parameters of the interaction network—connectance C (the fraction of realized species pairwise interactions) and modularity Q (the degree to which species are organized into densely interacting sub-communities)—affect the statistical properties of the attractors in the competitive Generalized Lotka–Volterra (GLV) model. We focus on the number of coexisting equilibria, extinction patterns, and the species abundance distribution (SAD), i.e., the distribution of abundances among surviving species at the final steady state.

As a reference case, analytical predictions for the onset of multistability and chaos in fully connected, unstructured networks ($C = 1$, $Q = 0$) [3] are compared with our numerical results. Using Monte Carlo simulations, we then assess how structured topology modifies these transitions.

The numerical results indicate that final state properties are substantially affected by network topology in competitive Lotka–Volterra models. In particular, some non-trivial combinations of C and Q lead to distinct final states that are strongly dependent on initial conditions. Lower connectance favors species persistence in this model—more species survive overall—but skews the final abundance distribution toward a few dominant species, thereby reducing the community's effective biodiversity despite higher coexistence.

[1] R. M. May, Nature 238, 413–414 (1972).
[2] Allesina, S., Grilli, J., Barabás, G. et al., Nat Commun 6, 7842 (2015).
[3] G. Bunin, Phys. Rev. E 95, 042414 (2017).

P30

Understanding How Turbulence Affects Contaminant Release from Sediment

C. C., Ng [1]

[1] *China-ASEAN College of Marine Sciences (CAMS), Xiamen University Malaysia (XMUM), Selangor Darul Ehsan, Malaysia.*
chuckchuan.ng@xmu.edu.my, chuckchuan.ng@gmail.com

Heavy metals such as cadmium (Cd), lead (Pb), copper (Cu), and zinc (Zn) commonly accumulate in river and coastal sediments and serve as important indicators of environmental pollution and ecological risk. Previous environmental monitoring research has focused on measuring these sediment-associated contaminants and identifying pollution hotspots. However, such assessments often treat sediments as relatively static systems and primarily rely on total contaminant concentrations, overlooking the physical processes that govern contaminant mobility.

This project is motivated by the hypothesis that water turbulence plays a critical role in determining whether sediment-bound contaminants remain trapped or are released into the water column. By driving sediment resuspension and particle transport, different flow conditions may alter contaminant mobility, bioavailability, and ecological risk. Despite its potential importance, this physical dimension remains insufficiently integrated into conventional environmental pollution studies.

To investigate this hypothesis, the proposed research will combine existing environmental datasets with concepts from fluid dynamics, controlled laboratory experiments, and computational modelling to better understand contaminant transport under different hydrodynamic conditions. Although heavy metals are used as a model contaminant system, the proposed framework is expected to be broadly applicable to other sediment-associated contaminants. By bridging environmental science and fluid dynamics, this interdisciplinary research aims to provide a more mechanistic understanding of contaminant transport and support improved predictive tools for environmental monitoring and sustainable management of aquatic ecosystems.

P31

Estimation of Optical Properties of Biological Tissues Using Quantitative Photoacoustic Imaging

Ngo Bamal Josephine[1]

[1]*University of Yaounde I, Cameroon*

Quantitative photoacoustic imaging (QPAI) is a hybrid modality combining the high spatial resolution of ultrasound with the strong optical contrast of light-based imaging. It enables the non-invasive estimation of physiological tissue parameters, such as absorption and scattering coefficients.

In this work, we develop a 2D Monte Carlo (MC) model to simulate light propagation in biological tissues and the resulting photoacoustic signals from hemoglobin absorption. The inverse problem of recovering optical properties is solved using a gradient descent optimization approach. The model successfully estimated absorption and scattering coefficients with relative errors below 2% compared to ground-truth values.

Our results demonstrate that computational modeling combined with stochastic simulations and inverse problem techniques can reliably quantify optical properties, providing a foundation for biomedical applications. Such quantitative measurements have potential applications in identifying pathologies including polycythemia vera (elevated hemoglobin absorption) and anemia (reduced hemoglobin absorption).

This study highlights the relevance of computational and modeling approaches in complex biological systems and illustrates the power of quantitative photoacoustic imaging as a tool for precision diagnostics.

Keywords: Quantitative photoacoustics, Monte Carlo simulations, inverse problems, optical properties, computational modeling, chromophore, hemoglobin.

P32

HARNESSING SOLAR ENERGY USING PARABOLIC DISH CONCENTRATOR FOR CLAY BRICK DRYING.

Morris Mutegi Nthieri[1], Millien Kawira Erastus[1], and Stephen Maina Njoroge[2], Joyce kagendo Nthiiri[3]

[1]Department of Physical Sciences, University of Embu, Embu, Kenya, [2]Department of Biological and Physical Sciences, Karatina University, Karatina, Kenya, [3]Department of Mathematics, Masinde Muliro University of Science and Technology, Kenya.

Parabolic dish solar concentrator (PDSC) is used for high-temperature applications because it focus solar flux to central point. High concentration ratios of 1000-3000 in PDSC makes them achieve high temperatures of 750-1000 ^{0}C. This study investigated the use of solar energy for drying clay bricks using a parabolic dish solar concentrator and a fiberglass-insulated metallic kiln. Mitigating air pollution and greenhouse gas emissions associated with the firing process in conventional methods. The study began by modeling, simulating and later experimental workout. Model blocks that included the sun, a parabolic dish, a receiver, a kiln, clay bricks, a fan, a dehumidifier, and sensors were developed, and simulation was run in MATLAB. The simulation was run for six days monitoring compressive strength, modulus of rupture, water absorption and other physical quantities. In the first two days the temperature was maintained at 50^{0}C using Arduino uno to prevent warping and cracking of the clay bricks. The aluminum foil reflector on the parabolic dish focused solar flux onto a spiral receiver at the PDSC focal point, where the absorbed thermal energy heated the air passing through the receiver. Hot air was blasted into a kiln housing damp clay brick, and after heat absorption, the air was withdrawn from the kiln via forced convection created by a fan. The extracted air was dehumidified to remove moisture and then recycled back to the receiver for reheating. Compressive strength was tested in day 7 as 5.37 N/mm², day 28 as 7.60 N/mm² and day 56 as 10.67 N/mm². Flexural strength increased from 1.03 N/mm² on day 7 to 1.43 N/mm² on day 28 to 1.83 N/mm² on day 56. Water absorption decreased from 26.67% on day 7 to 20.33% on day 28 and finally 18.33% on day 56. After 7 days, the solar drying method demonstrated a better performance compared to 30 days of the conventional drying method used in Mbeere, Embu, Kenya, with a 39.2% increase in compressive strength, underscoring its efficiency and effectiveness with a reduced time frame.

[1] Abid, M., Khan, M. S., & Ratlamwala, T. A. H. (2018). Techno-environmental analysis of a parabolic dish assisted recompression with and without reheat s-CO2 Brayton cycle. *International Journal of Exergy*, *27*(4), 527–552. https://doi.org/10.1504/IJEX.2018.096014

[2] Abreham, R. E., Getie, M. Z., & Demissie, Y. A. (2024). Recent Developments on Design and Thermal Performance Enhancement of Parabolic Dish Solar Concentrators: A Review. In K. Mequanint, A. K. Worku, M. Z. Getie, & Z. G. Workineh (Eds.), *Sustainable Development Research in Materials and Energy: Advancement of Science and Technology* (pp. 177–188). Springer Nature Switzerland. https://doi.org/10.1007/978-3-031-69860-6_11

P33

Abstract

The operational stability and performance of ambient-air-processed perovskite solar cells are strongly influenced by defects, moisture uptake, ion migration, and non-radiative recombination at device interfaces. This study investigated the effects of formamidinium iodide (FAI) and bathocuproine (BCP) interlayers in planar p-i-n $MAPbI_3$ perovskite solar cells with an ITO/PEDOT:PSS/$MAPbI_3$/PCBM/Ag architecture. Devices were fabricated by solution processing and thermal annealing, while complementary SCAPS-1D simulations were used to compare the control architecture with devices containing FAI, BCP, and combined FAI/BCP interlayers. The fabricated device achieved an experimental power-conversion efficiency of 9.89 %, with an open-circuit voltage of 1.0125 V, a short-circuit current density of 27.796 mA cm^{-2}, and a fill factor of 35.14 %. Simulated interface modification increased the efficiency from 10.00 % for the control device to 10.92 % with FAI and 11.02n% with BCP. FAI produced the highest fill factor, reaching 46.06 %, indicating improved interfacial charge extraction and reduced transport losses. BCP delivered the highest open-circuit voltage of 1.0124 V and the highest simulated efficiency, suggesting improved electron-contact selectivity and reduced interfacial recombination. The combined FAI/BCP device achieved a fill factor of 46.08 % and an efficiency of 10.92 %, although its voltage response indicates that further optimization is required. Quantum-efficiency results remained high across the visible region, with only small differences in short-circuit current density among the simulated devices. These findings demonstrate that FAI and BCP provide distinct interfacespecific benefits and offer a promising route for improving the performance and potential stability of ambient-air-processed perovskite solar cells. Further work should optimize the interlayer thicknesses and validate long-term stability through stabilized-efficiency, hysteresis, shelf-life, and thermal-ageing measurements.

P34

Performance comparison of different entropy measures in automated cancer image classification

Samuel T. Ogunjo [1]

[1]*Department of Physics, Federal University of Technology Akure, Ondo State, Nigeria*

Entropy-based measures have emerged as powerful tools for quantifying complexity and irregularity in medical images, offering potential for automated cancer diagnosis. However, the relative performance of different entropy formulations in histopathological image analysis remains insufficiently characterized. This study systematically compares four entropy measures—Permutation Entropy (Pent), Tsallis Entropy (Tent), Weighted Entropy (Went), and Rényi Entropy (Rent)—for classification of cancer histopathological images across tumor types, malignancy classes (benign vs. malignant), and magnification levels. Four entropy metrics were computed from histopathological image datasets and evaluated for their discriminatory power using ANOVA and t-tests. Performance was assessed based on classification accuracy (mean), consistency (standard deviation), and inter-metric correlation. Statistical significance was determined at $p < 0.05$. Permutation Entropy demonstrated superior overall performance (mean = 0.918) and highest consistency (std = 0.022) across all evaluation criteria. All four entropy measures showed statistically significant discrimination between benign and malignant classes ($p < 0.0001$), across tumor types ($p < 0.0001$), and magnification levels ($p < 0.0001$). Strong correlations were observed between Tent-Rent ($r = 0.987$), Pent-Tent ($r = 0.896$), and Pent-Rent ($r = 0.863$), indicating complementary information content. Magnification level significantly affected entropy values, with Went showing the strongest sensitivity ($F = 249.522$, $p < 0.0001$). Permutation Entropy emerges as the most robust and consistent metric for histopathological cancer image classification, though the high correlation between Tent and Rent suggests potential redundancy. The significant magnification dependence of all metrics underscores the importance of standardized imaging protocols in entropy-based diagnostic workflows. These findings provide evidence-based guidance for selecting entropy measures in automated cancer diagnosis systems.

AI agents system for automatic ICD predication

Dr. Khaled Omar

Damascus Univeristy

Syria, Damascus

Abstract

International classification of Diseases (ICD) is a standard coding of the diseases which approved from the world health organization (WHO), also the medical claim ICD coding is essential step in the medical insurance companies , this coding process need many resource (time and human) , and also this process must be very accurate because any error in the coding process will led to loss in the revenue, many systems and algorithms have been developed to make this process automatic or semi-automatic, these systems and algorithms were depends on many technologies, in this paper we have developed an automatic system for medical claims ICD generation , this developed system contains several artificial intelligent agents (AI Agents), also the coding agent which generate the claim primary ICD code and list of secondary ICD codes , contains many ICD code generation layers , the vector database search layer, features layer, Large language model layer , patient history layer, also this developed system contains cache layer for handling duplicated requests , and feedback layer to make this system with continuous learning from the user feedback, we have tested this system and its accuracy was above 95%.

P36

Abstract template for Hands-On Research in Complex Systems School

Sapia Marco[1], Kaczer Laura[2], Bavassi Luz[1]

[1]LABORATORIO DE NEUROCIENCIAS DE LA MEMORIA (IFIBYNE, UBA-CONICET, ARGENTINA).

[2]LABORATORIO DE LENGUAJE Y COGNICIÓN (FBMC, FCEN,UBA, ARGENTINA)

Despite significant advances in neuroscience, the complex mechanisms underlying overall brain function remain not fully understood. Traditionally, neural processing has been studied by focusing on specific regions of activation using classical univariate techniques. To address this limitation, this work aims to contrast these well-established methods with emerging multivariate approaches, such as Representational Similarity Analysis (RSA), which seek to understand the brain's activity as a distributed, interconnected network rather than isolated regional activations. Within this framework, this study investigates how semantic context modulates word processing by evaluating its behavioural and neurophysiological effects. We implemented a free association protocol where participants responded to word stimuli presented in either semantically homogeneous or heterogeneous blocks. To evaluate these effects, we measured neural activity using EEG and analyzed the semantic similarity of the behavioural responses using fastText, a language model based on word embeddings. For the neural data, we compared a classical univariate Event-Related Potential (ERP) approach with the aforementioned multivariate RSA technique. The results were favourable for both the behavioural analysis and the classical univariate technique, successfully detecting a significant contextual modulation in both domains. Specifically, the univariate analysis revealed significant differences between conditions within the N400 time window, a neural marker classically studied in sentence incongruity paradigms [1]. In contrast, the current application of the multivariate RSA approach has not yet detected significant categorical differentiation in the neural signal. These findings confirm that context modulates semantic processing at both behavioural and classical electrophysiological levels, while highlighting the need for further exploration and refinement of multivariate neural representations

[1] Kutas, M., & Hillyard, S. A. (1980). Reading senseless sentences: Brain potentials reflect semantic incongruity. *Science*, 207(4427), 203-205.

P37

Abstract template for Hands-On Research in Complex Systems School

Sedofeito, C.[1], Flores, M [1], Melissari, B. [1], Gallot, T.[1], Aichele, J.[2],Boué, P.[3], Roux, P.[3]

[1] *Instituto de Física, Facultad de Ciencias, Universidad de la República, Iguá 4225, Montevideo, Uruguay*

[2] *Institut für Geophysik, ETH Zürich, Sonneggstrasse 5, 8092 Zürich, Switzerla*

[3] Institut de Science de la Terre, Université Grenoble Alpes, 1381, rue de la Piscine, Gieres, France

Glacial tills are water-saturated, heterogeneous granular sediments that accommodate the basal motion of glaciers and ice streams through a combination of stick-slip, distributed shear, and pore-pressure-driven slip migration. Field observations from Whillans Ice Stream and other sites show that till deformation is episodic and strongly analogous to fault-gouge rupture, yet its micro-mechanical controls such as force-chain failure, grain crushing, velocity-weakening friction, and the transition toward a fractal grain-size distribution documented by [1] cannot be directly observed in situ. Here we apply the ultrafast ultrasonic imaging framework developed by [2], [3], [4] and [5] to probe controlled laboratory ruptures on a granular fault analogue, using a horizontal imaging geometry that places the probe on a plane parallel to the fault interface. An elastic sample is pre-stressed over a glass plate, with a single layer of angular limestone ranging from 1 to 5 mm, simulating the gouge. The interface is sheared at constant velocity while a Verasonics Vantage scanner coupled to a 5-MHz linear array records the 2D displacement field at 2000 fps. This fault-parallel configuration gives sub-wavelength access to the rupture and allows direct tracking of the nucleation phase, the propagating rupture front, and the radiated shear wavefield, complementing the fault-perpendicular geometry used in previous work.

Across experiments we image stick-slip events, preceded by systematic decorrelation precursors attributed to force-chain rearrangement in the granular layer [6, 7]. The wavefield is consistent with a double-couple (DC) source mechanism for sub-Rayleigh ruptures under weak bi-material contrast, as reported by [4] and [5], with a single-force contribution near the interface; the radiated pattern, the negative ISO component associated with compaction [8]. Interpreted within the till framework of [9] and [10], the observed precursory grain rearrangement and DC radiation, provide a laboratory analogue for the basal icequakes [11] generated at sticky spots on the ice–till interface [12], where over-consolidated gouge fails in rate-weakening shear [13]. The fault-parallel ultrasonic geometry thus offers a near-field, grain-scale window onto the same physics that governs glacial till slip, and establishes a calibration path between laboratory signatures and field icequakes.

[1] N. R. Iverson, T. S. Hoover, R. LeB. Hooke, Ann. Glaciol. **22**, 167 (1996).
[2] S. Latour, A. Schubnel, S. Nielsen, R. Madariaga, S. Vinciguerra, Geophys. Res. Lett. **40**, 5064 (2013).
[3] J. Aichele, *Rupture dynamics of laboratory-scale granular fault experiments*, PhD Thesis, ETH Zürich (2019).
[4] J. Aichele, B. Giammarinaro, M. Reinwald, G. Le Moign, S. Catheline, Front. Earth Sci. **8**, 129 (2020).
[5] J. Aichele, S. Catheline, P. Roux, J. Geophys. Res. Solid Earth **129**, e2023JB027336 (2024).
[6] P. A. Johnson, B. Ferdowsi, B. M. Kaproth, M. Scuderi, M. Griffa, J. Carmeliet, R. A. Guyer, P.-Y. Le Bas, D. T. Trugman, C. Marone, Geophys. Res. Lett. **40**, 5627 (2013).
[7] G. Michlmayr, D. Cohen, D. Or, J. Geophys. Res. Solid Earth **118**, 6086 (2013).
[8] Z. Song, G. Kwiatek, P. Martínez-Garzón, G. Dresen, Geophys. Res. Lett. **52**, e2024GL113093 (2025).

[9] A. Damsgaard, J. Suckale, L. Goren, arXiv:2002.02436 (2020).
[10] Z.-X. Zeng, L.-M. Zhang, Z.-D. Xu, M. Kamali Zarch, Acta Geotech. **19**, 4809 (2024).
[11] T. S. Hudson, A. M. Brisbourne, F. Walter, D. Gräff, R. S. White, A. M. Smith, J. Geophys. Res. Earth Surf. **125**, e2020JF005627 (2020).
[12] S. Anandakrishnan, R. B. Alley, Geophys. Res. Lett. **24**, 265 (1997).
[13] B. P. Lipovsky, E. M. Dunham, J. Geophys. Res. Earth Surf. **122**, 973 (2017).
[14] R. T. Cerbus, L. Brivady, T. Faug, H. Kellay, arXiv:2406.14810 (2024).

P38

Dynamical Behaviors Of Vertical-Cavity Surface-Emitting Lasers With An Embedded Saturable Absorber Subjected To An On-Off Keying (OOK) Current Modulation

L. P. G. Temgoua [1] , **J. H. Talla Mbé** [1,2] , **and P. Woafo** [1]

[1]Laboratory of Modeling and Simulation in Engineering, Biomimetics, and Prototypes, Department of Physics, University of Yaoundé I, PO Box 812, Yaoundé, Cameroon

[2] Research Unit of Condensed Matter, Electronics and Signal Processing, Department of Physics, University of Dschang, PO Box 67, Dschang, Cameroon

We numerically study the dynamics of vertical-cavity surface-emitting lasers with an embedded saturable absorber (VCSEL-SA) when modulated by current [1, 2] in the form of an analog on-off keying (OOK) [3]. It is found that the laser gives a pulse-like response when operated below the threshold current. After the threshold current, which is in the excitable phase, the laser generates single spikes (phasic spiking) [4, 5] and a series of spikes (tonic spiking) [6, 7] wherein the amplitude of the spikes varies as the form of the current. Complex dynamics such as bursting oscillations and chaotic dynamics are successfully generated at low frequencies (few MHz) where it is not usually expected. After this excitable phase, the laser copies the OOK current with underdamped oscillations generated during the OFF phase of the OOK current.

[1] A. Hurtado, J. Javaloyes, Appl. Phys. Lett. **107**, 241103 (2015).
[2] M. A. Nahmias, B. J. Shastri, A. N. Tait and P. R. Prucnal, IEEE J. Sel. Top. Quantum Electron. **19**, 1800212 (2013).
[3] S. Bharati, M. A. Rahman, P. Podder, *arXiv preprint arXiv:2002.03601* (2020).
[4] F. Peper, K. Leibnitz, J. N. Teramae, T. Shimokawa, N. Wakamiya, IEEE internet of things Journal. **3** 49-58 (2016).
[5] L. Wang, Y. H. Qiu, Y. Zeng, Front. Comput. Neurosci. **10**, 102 (2016).
[6] J. Robertson, E. Wade, Y. Kopp, J. Bueno, A. Hurtado, IEEE J. Sel. Top. Quantum Electron. **26**, 1–15 (2019).
[7] J. Robertson, E. Wade, A. Hurtado, Electronics. **25** 1–7 (2019).

P39

Improving the Performance of Perovskite Solar Cells Using Double PEDOT:PSS Layer

Kufre I. Udofia, Izuchukwu K. Nwokolo, Peverga Rex Jubu, Aaron O. Aransiola, Amakom C, Adamu A. Goje, Kanayo L. Oguzie, Ikechukwu I. Ayogu, Chinyere A. Madu, Emeka E. Oguzie

Africa Center of Excellence in Future Energies and Electrochemical Systems (ACE-FUELS), Federal University of Technology, Owerri, Nigeria

Abstract:

Inverted perovskite solar cells are often limited by interfacial recombination, inefficient charge extraction, and resistive losses at the charge-transport interfaces. In this study, a double-layer poly(3,4-ethylenedioxythiophene): polystyrene sulfonate (PEDOT:PSS) hole-transport layer was investigated as an interfacial engineering strategy to improve charge transport and device performance. Inverted perovskite solar cells with an ITO/PEDOT: PSS×2/$MAPbI_{3-x}Cl_x$/$PC_{70}BM$/Ag architecture were fabricated and characterised by spin coating. SCAPS-ID simulations were employed to evaluate the effects of carrier density, interfacial properties, and resistive losses. The fabricated device exhibited an open-circuit voltage (V_{OC}) of 1.01 V, short-circuit current density (J_{SC}) of 19.68 mA cm^{-2}, fill factor (FF) of 27.96% and power conversion efficiency (PCE) of 5.6 %. SCAPS-ID simulation predicted a PCE of 6.16 %, indicating further potential for performance improvement. The results identify contact resistance and interfacial recombination as major factors limiting device efficiency. Simulation analysis further showed that device performance is favoured by reduced series resistance, increased shunt resistance, and appropriate control of carrier density.

P40

Cell-inspired shape adaptation of flexible active matter under confinement

C. G. Vidales-Hernández[1] , JL Carillo-Estrada[1,2] , and F. Donado[2]

1 Instituto de Física, Benemérita Universidad Autónoma de Puebla, Puebla 72570, México

2 Instituto de Ciencias e Ingeniería, Universidad Autónoma del Estado de Hidalgo, Pachuca Hidalgo 42184, México

White blood cells dynamically adapt their shape while chasing pathogens under blood flow conditions. Inspired by this behaviour, we ask how similar active agents respond to complex confinement and obstacle interactions. We addressed this question with a macroscopic-scale experimental model: Flexible superstructures composed of self-propelled robots enclosed within a flexible membrane. Then, we let them move within networks of rounded regions connected by narrow channels. It is observed that the superstructure passes through channels narrower than itself and even unclogs them when partially filled with soft and wet granular particles, due to its flexibility and morpho-adaptability. We characterized their motion using mean square displacement and effective diffusion coefficient and found that both dynamical properties are related to the internal arrangement of its inner robots, while the unclogging process also increases the granular medium's local order. This work could establish a first step toward a table-top model with promise for capturing the basic dynamical features of white blood cell motion.

[1] C.G. Vidales-Hernández, JL Carrillo Estrada, F. Donado, On the motion of self-propelled flexible superstructures in complex networks, Submitted for publication (Jan, 2026).
[2] G. Chacón-Acosta, A. León-Ramírez and O. González-Gaxiola, Phys. A Stat. Mech. Appl. 628, 129155 (2023).
[3] Salvermoser M, Begandt D, Alon R and Walzog B, Frontiers in inmmunology (2018)
[4] A. Caspi, R. Granek and M. Elbaum, Phys. Rev. Lett. 85, 5655 (2000)
[5] J. F. Boudet, J. Lintuvuori, C. Lacouture, T. Barois, A. Deblais, K. Xie, S. Cassagnere, B. Tregon, D. B. Brückner, J. C. Baret and H. Kellay, Sci. Rob. 6, eabd0272 (2021)
[6] M. C. Gandikota and A. Caccicuto, Soft Matter 19, 315 (2023)

P41

QUANTITATIVE CT IMAGE QUALITY ASSESMENT: EXPERIMENTAL VALIDATION OF OPEN-SOURCE TOOL USING ADVANCED CHARACTERIZATION METRICS

Villagrán C. Author[1], **Gómez D. Author**[1,2]

[1]Universidad del Valle de Guatemala, Guatemala
[2]Nuclear Applications Area – Ministry of Energy and Mines (MEM), Guatemala
(Presenting author underlined)

Quantitative assessment of image quality in computed tomography (CT) is essential for ensuring reliable diagnostics while optimizing the trade-off between spatial resolution, noise, and patient dose [1]. This need is particularly critical in resource-limited healthcare systems, where access to validated and cost-effective tools remains limited. In this work, we present a hands-on experimental and computational framework for CT image quality evaluation, with a focus on validating an accessible software solution for public hospitals in Guatemala.
Using the ACR CT Accreditation Phantom, we experimentally estimated key image quality metrics, including the task transfer function (TTF), noise power spectrum (NPS), and detectability index (d'), following AAPM TG-233 recommendations [1,2]. Data acquisition was performed under controlled variations of imaging parameters to explore system response across different conditions.
To ensure reliability and accessibility, the software ImQuest, free version, was evaluated alongside an independent, reproducible analysis pipeline developed using ImageJ macros and Python-based signal processing [8]. The slanted-edge method was employed for longitudinal spatial resolution estimation [6,7], while an alternative spectral approach based on point spread function (PSF) reconstruction from submillimetric bead inserts in the phantom was implemented for cross-validation. Additionally, a Monte Carlo-based approach was introduced to propagate uncertainties in spatial resolution metrics, providing a statistical characterization of variability.
Results show strong agreement between both pipelines in terms of TTF and NPS behavior [5], as well as consistent detectability trends [3,4]. The detectability index correlates with the perceptual visibility of low-contrast objects in the phantom, particularly near the 5 mm scale, highlighting the link between physical metrics and observer performance.
This work demonstrates a reproducible and modular framework for CT image quality evaluation, integrating experimental techniques, numerical modeling, and image analysis. It further supports the feasibility of implementing validated, low-cost computational tools for quality assurance in public healthcare systems, contributing to improved diagnostic reliability in resource-constrained settings.

References

[1] E. Samei et al., *Med. Phys.* **46**, e735–e756 (2019).
[2] J. M. Wilson et al., *Med. Phys.* **40**, 031908 (2013).
[3] S. Richard et al., *Med. Phys.* **39**, 4115–4122 (2012).
[4] B. Chen et al., *Med. Phys.* **41**, 071909 (2014).
[5] K. L. Boedeker et al., *Phys. Med. Biol.* **52**, 4027–4046 (2007).
[6] C. Anam et al., *J. Appl. Clin. Med. Phys.* **19**, 244–252 (2018).
[7] S. N. Friedman et al., *Med. Phys.* **40**, 051907 (2013).
[8] J. Solomon et al., *Med. Phys.* **45**, e134 (2018).

P42

Multi-scale simulations reveal differences between dusty plasma and hydrodynamic turbulence

Rauoof Wani [1] , **and Sanat Tiwari** [1]

[1]*Department of Physics Indian Institute of technology Jammu, Jammu 181221, India*

Dusty plasmas are complex plasma systems containing micron- or nanometer-sized solid particles that acquire huge ($10^4 - 10^5$ e) electric charge and interact with electrons, ions, and other dust particles. Because the dust particles can interact strongly with one another, dusty plasmas provide a unique environment for studying collective behavior, nonlinear dynamics, and transport processes at the microscopic level. They are found in a variety of natural environments, including planetary rings, cometary tails, and interstellar clouds, and can also be generated under controlled laboratory conditions. When the interparticle coupling becomes strong, the dynamics can no longer be described adequately by conventional weakly coupled plasma or classical fluid models, and the role of particle correlations and viscoelasticity becomes important.

In this work, we investigate turbulence in strongly coupled dusty plasmas using large-scale molecular-dynamics simulations. The dust particles interact through a screened Coulomb (Yukawa) potential. Turbulence is generated through large-scale forcing, and the resulting particle motion is analyzed over a broad range of spatial scales. We characterize the turbulent state using the kinetic-energy spectrum, velocity probability distributions, and higher-order velocity structure functions to investigate energy transfer and intermittency.

A key result of our simulations is that the kinetic-energy spectrum exhibits an approximate power-law scaling, $E(k) \sim k^{-7/2}$, which is substantially steeper than the classical Kolmogorov prediction, $E(k) \sim k^{-5/3}$. This difference indicates that the turbulent energy cascade in strongly coupled dusty plasmas is significantly modified compared with conventional fluid turbulence, with energy not being transferred efficiently toward smaller scales in the classical manner. We also observe non-Gaussian velocity fluctuations and the intermittency at smaller scales. The analysis further indicates that elastic and viscous contributions both play important roles in the evolution and dissipation of turbulent energy, reflecting the viscoelastic nature of the strongly coupled system.

These results provide a kinetic picture of turbulence in strongly coupled dusty plasmas and demonstrate how microscopic particle correlations can influence macroscopic turbulent transport. Understanding this modified energy cascade is important for describing energy and momentum transport in strongly coupled complex plasmas and may provide insight into turbulent processes occurring in laboratory and astrophysical dusty-plasma environments.

[1] Frish.U.(1995). Turbulence, the legacy of A.N Kolmogorov, Cambridge University Press.

[2] Rauoof Wani and Sanat Tiwari, “Intermittent viscoelastic turbulence in strongly coupled plasmas”, Physical Review Fluids, **1**, 043301 (2026).

[3] Rauoof Wani, Mahendra Verma and Sanat Tiwari, Phil. Trans. R. Soc. A (2026) **384** (2325): 20250026

P43

Understanding the Physical Mechanisms Driving Marine Heatwaves to Improve Predictions in West African Coastal Upwelling Regions

Dametoti Yamoula[1, 2*], Ifeoluwa Adebowale Balogun[1, 2], Bamol Ali Sow[3]
[1]West African Science Service Center on Climate Change and Adapted Land Use (WASCAL), Doctoral Research Program in West African Climate Systems,
[2]Federal University of Technology, Akure, Nigeria
[3]Laboratoire d'Oceanographie, des Sciences de l'Environnement et du Climat, Université Assane Seck de Ziguinchor, Senegal

*Corresponding author: yamoula.d@edu.wascal.org

Abstract
Understanding the mechanisms driving temperature variability is essential for improving predictions and assessing future climate risks, particularly in coastal upwelling systems because of their ecological and socioeconomic importance. This study investigates the ocean mixed-layer heat budget and wind-stress forcing as potential mechanisms driving marine heatwaves (MHWs) in the major coastal upwelling systems of West Africa. The results show distinct mechanisms between the two regions. In the Senegal-Mauritania Upwelling System (SMUS), MHWs are primarily associated with remote wind forcing, which plays a dominant role in modulating regional ocean temperature variability. In contrast, MHWs in the Gulf of Guinea Upwelling System (GGUS) are mainly driven by oceanic advection, while wind forcing plays a secondary role. These contrasting mechanisms highlight the regional dependence of MHW drivers and provide valuable insights into their predictability. The findings may contribute to the development of AI-assisted early-warning systems for improving MHW prediction and assessing future climate risks in these vulnerable coastal regions.